EFFECTS OF TOP-SOIL PROPERTIES ON SEISMIC DEFORMATIONS OF UNDERGROUND STRUCTURES

ALTYAPILARDA YÜZEY ZEMİNİ ÖZELLİKLERİNİN SİSMİK DEFORMASYON DAVRANIŞINA ETKİSİ

FATMANUR ERCİYES

PROF. DR. BERNA UNUTMAZ

Supervisor

Submitted to

Graduate School of Science and Engineering of Hacettepe University

as a Partial Fulfilment to the Requirements

for be Award of the Degree of Master of Science

in Civil Engineering

2024

To my beloved family…

ABSTRACT

EFFECTS OF TOP-SOIL PROPERTIES ON SEISMIC DEFORMATIONS OF UNDERGROUND STRUCTURES

Fatmanur ERCİYES

Master of Science, Department of Civil Engineering

Supervisor: Prof. Dr. Berna UNUTMAZ

July 2024, 64 pages

Underground structures have become an indispensable part of modern urban life, such as tunnels, metro stations and pipelines. As the design and construction of these structures evolve, their behavior during earthquakes has become an increasingly significant consideration. Contrary to above-ground structures, the earthquake response of underground structures is not controlled by the internal forces of the structure but by the ground with whom it is in interaction. In addition, the response of the structure is influenced by the structural parameters and the expected earthquake characteristics. In particular, the depth of burial is one of the main parameters affecting the seismic response of the structure. Experience shows that the behavior during an earthquake is relatively better with increasing depth. However, the effect of surface soil characteristics, defined as soil along the burial depth, on underground structure behavior has been relatively

understudied. The purpose of this study is to investigate the effect of changes in the strength and plasticity of the surface soil on the behavior of underground structures under earthquake excitation. For this purpose, one-dimensional soil response analyses were performed with different surface soil scenarios to determine the free field deformations, and the soil structure interaction response behavior in these scenarios was investigated by two dimensional pseudo-static analyses. In addition, to determine the dominant effects of surface soil properties on the behavior, the changes in shear wave velocity, shear strength and plasticity index, which are important parameters of the complex structures of cohesive soils, were focused on. The results of the investigations are a description of the variation of the racking coefficient, which is defined as the ratio of the differential deformation of the soil in free field conditions to the differential deformation experienced by the structure along its height, with different surface soil properties and the soil property that plays the dominant role in this variation.

Keywords: Soil-structure interaction, pseudo-static analysis, site response analysis, racking coefficient

ÖZET

ALTYAPILARDA YÜZEY ZEMİNİ ÖZELLİKLERİNİN SİSMİK DEFORMASYON DAVRANIŞINA ETKİSİ

Fatmanur ERCİYES

Yüksek Lisans, İnşaat Mühendisliği Bölümü

Tez Danışmanı: Prof. Dr. Berna UNUTMAZ

Temmuz 2024, 64 sayfa

Tüneller, metro istasyonları ve boru hatları gibi yeraltı yapıları modern kent yaşamının vazgeçilmez bir parçası haline gelmiştir. Bu yapıların tasarım ve inşa prensipleri geliştikçe, deprem sırasındaki davranışları daha önemli bir konu haline gelmiştir. Üst yapıların aksine, yer altı yapılarının depreme tepkisi yapının iç kuvvetleri tarafından değil, etkileşim içinde olduğu zemin tarafından kontrol edilir. Buna ek olarak, yapının tepkisi yapısal parametrelerden ve beklenen deprem özelliklerinden etkilenir. Özellikle gömülme derinliği yapının sismik tepkisini etkileyen ana parametrelerden biridir. Deneyimler, deprem sırasındaki davranışın derinlik arttıkça nispeten daha iyi olduğunu göstermektedir. Bununla birlikte, gömülme derinliği boyunca zemin olarak tanımlanan yüzey zemini özelliklerinin yeraltı yapısı davranışı üzerindeki etkisi nispeten az çalışılmıştır. Bu çalışmanın amacı, yüzey zemininin mukavemet ve plastisitesindeki değişikliklerin deprem uyarımı altında yeraltı yapılarının davranışı üzerindeki etkisini araştırmaktır. Bu amaçla, serbest alan deformasyonlarını belirlemek için farklı yüzey

zemini senaryoları ile tek boyutlu zemin tepki analizleri gerçekleştirilmiş ve bu senaryolardaki zemin yapı etkileşimi tepki davranışı iki boyutlu sözde statik analizler ile incelenmiştir. Ayrıca, yüzey zemini özelliklerinin davranış üzerindeki baskın etkilerini belirlemek için, kohezyonlu zeminlerin karmaşık yapılarının önemli parametreleri olan kayma dalgası hızı, kayma mukavemeti ve plastisite indeksindeki değişimlere odaklanılmıştır. Araştırmaların sonuçları, serbest arazi koşullarında zeminin farklı deformasyonunun yapının yüksekliği boyunca maruz kaldığı farklı deformasyona oranı olarak tanımlanan bükülme oranının farklı yüzey zemini özellikleriyle değişimini ve bu değişimde baskın rol oynayan zemin özelliğini tanımlamaktadır.

Anahtar Kelimeler: Yapı zemin etkileşimi, pseudo-statik method, zemin tepki analizi, bükülme oranı

ACKNOWLEDGMENT

As the end product of a master's degree that required migration from one city to another, this thesis would not have been possible without Prof. Dr. Berna UNUTMAZ and Prof. Dr. Mustafa ŞAHMARAN.

I would like to thank my supervisor, Prof. Dr Berna UNUTMAZ, who has always encouraged me and has inspired me with the person that she is.

I would like to thank Prof. Dr. Mustafa ŞAHMARAN for having faith in me and for giving me the opportunity to discover my potential.

I want to thank Assoc. Prof. Dr. Mustafa Kerem KOÇKAR and Assoc. Prof. Dr. Mustafa Abdullah SANDIKKAYA, with whom I feel very fortunate to have had the opportunity to participate in various scientific activities and to benefit from their deep theoretical and practical experience. I also thank Assoc. Prof. Dr. Ebru AKIŞ for her contribution in evaluating my thesis.

My parents, Emine and Mustafa ERCİYES, have always supported me to be where I am happy and to do what I am happy. I thank them for everything.

Finally, I would like to thank Bülent TURAN who has shared all the difficulties with me during my master’s studies, which I consider to be a fascinating journey.

Fatmanur ERİCYES

July 2024, Ankara

TABLE OF CONTENTS

LIST OF FIGURES

LIST OF TABLES

SYMBOLS AND ABBREVIATIONS

Symbols

$\partial u/\partial t$	The particle velocity
$\partial^2 u/\partial t^2$	The particle acceleration
a_s	The maximum grain acceleration
ϵ_l	The axial or longitudinal strain
ϵ_{lm}	The peak value of the axial or longitudinal strain
c_p	P-wave velocity
c_s	S-wave velocity
V_p	The peak grain velocity
V_s	The maximum particle velocity
γ_m	Shear strain induced by the S-wave
$1/\rho_m$	Curvature
φ	Angle of S- or P-waves during seismic event
G/G_{max}	Shear modulus degradation
τ	Simple shear stress
γ	Shear strain
G	Shear modulus of soil
Δ	Shear deflection over structural height
H	Hight of structure
L	Width of the structure
P	Concentrated force
S_1	Force required for unit racking deformation

F	Fexibility ratio
I_R	Moment of inertia of slabs
I_W	Moment of inertia of the sidewalls
E	Elastic modulus
R	Racking coefficient
$\gamma_{free-field}$	Shear strain in free-field condition
$\gamma_{structure}$	Shear strain of the structure
$\tau_{structure}$	Shear stress acting on the structure
θ	Normalised mean rotation
c'	Drained shear strength
c_u	Undrained shear strength
E'_s	Drained modulus of deformation
E_u	Undrained modulus of deformation
β'	Correction coefficient
δ	Soil density
V_s	Shear wave velocity
EI	Bending stiffness
EA	Axial stiffnes
F	Unit load causing unit deformation
G_{rep}	Representative shear modulus
ζ	Damping ratio of the soil
γ_c	Cyclic shear strain
f_{max}	Target frequency
m	Parameter representing the stress-dependent stiffness
υ	Poisson's ratio

c	Failure criteria shear strength
φ	Shear resistance angle
ψ	Dilatancy

Abbreviations

1D	One Dimensional
2D	Two Dimensional
EC8	Eurocode 8
EQ	Earthquake
FE	Finite Element
FEM	Finite Element Method
EL	Equivalent Linear
FHWA	Federal Highway Administration
NCHRP	National Cooperative Highway Research Program
PEER	Pacific Earthquake Engineering Research
PGA	Peak Ground Acceleration
PGV	Peak Ground Velocity
PI	Plasticity Index
GRA	Ground Response Analysis
TBEC	Turkish Building Earthquake Code
SS	Surface Soil

1. INTRODUCTION

1.1. Research Statement

As urban life evolves, needs such as traffic control and underground utilities have led to rapid developments in the principles for designing and constructing underground structures. In parallel with this development, the seismic evaluation and design principles of these structures have also been the subject of research.

Traditionally, substructures are considered to perform better than superstructures (Sharma and Judd, 1991). However, cases such as the Daikai metro station, which completely collapsed in the Hyogoken-Nambu (Kobe) earthquake even though it was not located on an active fault line and there was no phenomenon such as liquefaction, have shown that infrastructure can completely collapse due to earthquake effects (Iıda et al., 1996, Noshida and Nakamura, 1996).

The literature shows that the behavior of these structures, which usually interact with the ground in at least three directions, is significantly modified by the surrounding soil (Wang, 1993; Hashash et al., 2001). In addition, structural embedment depth, stiffness difference between soil and structure, structure size and shape characteristics are other parameters influencing the response (Shawkyi and Koichi, 1996; Hashash et al., 2001; Huo et al., 2005; Tsinidis et al., 2020).

Buried depth has been shown to significantly alter structure behaviour (Sharma and Judd, 1991). The effect of the soil surface along the depths of the burials is not well understood. The present study focuses on the earthquake response of a single-span rectangular structure buried in a cohesive soil with different surface soils. Pseudo-static analysis is used to evaluate the performance of subsurface structures in seismic events. Pseudo-static analysis is more effective than dynamic analysis, which requires complex input parameters and extensive computations (Wang, 2001; Huo, 2005; Hashash, 2010; Pitilakis and Tsinidis, 2010; Yang et al., 2023). In addition, one-dimensional soil

response analyses have also been used to assess the behavior of the soil under free-field conditions without any structure.

1.2. Research Objective

The objectives of this study can be listed in the following way;

- The description of the change in seismic deformation behaviour of the sub-surface structural system as a result of change in surface soil,
- Analysis of parameters that dominantly influence the response behavior of the surface soil from the strength and plasticity properties.

1.3. Outline of Thesis

This thesis study consists of four main headings. The contents of these chapters can be explained as follows;

Chapter 1 provides an introduction to the subject of the thesis and states the study objectives.

Chapter 2 provides a detailed overview of the infrastructure earthquake design processes and the literature on the parameters that influence seismic behaviour.

Chapter 3 provides detailed information on the materials and methods used in the study. In addition, one-dimensional response analyses and two-dimensional structure-soil interaction analyses are presented in this chapter.

Chapter 4 presents a comparative evaluation of the effect of different properties of the surface soil on the response of the infrastructure as a result of the analyses performed.

Chapter 5 concludes findings of parametric study and makes proposals for subsequent studies.

2. LITERATURE SURVEY

2.1. Seismic Considerations of Underground Structures

A summary of earthquake safety assessment of subsurface systems and a review of the literature on the subject are presented in this chapter.

The term underground structure is used to describe structures such as tunnels, pipelines and mining structures. The main difference between these structures and superstructures is that their dimensions in the longitudinal direction are much greater than their dimensions in the cross-sectional direction. In addition, the principles of seismic behavior of underground structures can be clearly distinguished from those of superstructures. This is mainly because underground structures usually interact with the ground in at least three directions. For the majority of buried installations, the inertia of the surrounding mass is much greater than the structural inertia. This means that the earthquake response of structures below ground is determined and controlled by the seismic response of the surrounding ground, rather than by their own internal forces, as in the case of superstructures. The surrounding ground dominates the earthquake performance of the buried facility (Hashash et al., 2001).

In this thesis, the term underground structure is used to represent metro stations and tunnels with rectangular cross-sections.

The first observations on the response of subsurface engineering works to earthquakes were made by Sharma and Judd (1991), who interpreted 192 reports that included observations on the behaviour of subsurface engineering works in 85 earthquakes around the world. In this study, it was concluded that underground structures suffered significantly less damage in earthquakes than superstructures, that the observed damage decreased with increasing depth of burial of underground structures, and that systems in the soil environment suffered more damage than those in the rock environment.

Underground structures were considered safer than superstructures against the effects of earthquakes until the Hyogoken-Nambu (Kobe) earthquake of 17 January 1995. However, this earthquake was the first time that a subway station completely collapsed due to an earthquake, and it was realized that seismic effects should be considered in designing of subground facilities. The M_w=6.9 quake caused the failure of over half of the structure's central columns, the top slab collapsed, and excessive deformation was observed in the ground above the station (see Figure 1 and Figure 2). Analysis of the damage patterns observed in the station structure indicated that large horizontal forces had been transmitted to facility from adjacent soil. The collapse of facility was a result of the relative deformation between the floor and ceiling levels during the earthquake and the transfer of excessive internal forces from the floor to the ceiling slab. The Daikai subway station is a unique case in that it is the first underground structure to completely collapse due to an earthquake without liquefaction (Iıda et al., 1996).

Figure 1. Damage to the central columns of Daikai Station (Uenishi and Sakurai, 2000)

Figure 2. Severe deformation observed as a result of Daikai Station collapse (Uenishi and Sakurai, 2000)

The Daikai subway station was designed to withstand the normal load of surface ground, lateral ground forces and structural weight of the frame. However, as was common practice at the time of the station's construction, seismic loads were not considered in the design (Iıda et al., 1996). As a result of analytical investigations, the collapse mechanism of the station structure was explained as the additional bending moment and shear force transmitted from the ground to the structure causing relative deformation between the upper and lower slabs, and the weight of the surface soil causing the structure to exceed the design loads and then to collapse (Noshida and Nakamura, 1996). It was also thought that the thickness of the surface soil might have an effect on the damage mechanism, since other underground structures that experienced the same earthquake, those buried deeper, suffered relatively less damage. However, since the load-transferring mechanism between the overburden and the top slab could not be explained with the information available at the time, the effect of the overburden on collapse could not be described (Iıda et al., 1996).

This thesis focuses on the impact of surface geotechnical properties on the earthquake deformation behaviour of subsurface facilities.

2.2. Philosophy and Approaches used for Assessing Dynamic Behavior of Underground Structures

Limiting the performance of subsurface installations by surrounding ground requires different methods to those used in superstructure design. The surrounding soil prevents the underground structure from oscillating independently of the surrounding environment (Wang, 1993; Hashash et al., 2001).

Wang (1993) proposed a deformation method for underground structures, which have different behavioral characteristics from superstructures. The deformation technique is founded on the principle that the underground structure has sufficient ductility to adapt to the deformations induced by the earthquake and transferred from the surrounding soil. Such structures are more sensitive to earthquake-induced deformations. Therefore, this thesis focuses on the deformation method.

Çilingir and Madabhusi (2011) investigated the earthquake response of square-section shallow tunnels embedded in sandy grounds through a series of dynamic centrifuge tests and finite element analyses. As a result of the experiments and complementary numerical analyses, they reported that the dynamic response of square section tunnels consisted of three phases: an initial transient phase, subsequent steady state cycles, and a residual static phase. Accordingly, it was observed that most of the plastic deformation occurred in the first cycles of the earthquake motion. In the following cycles, the plastic deformation in the tunnel decreased compared to the first cycles (see Figure 3 for measured earth pressures in the stages and the experimental setup). However, a racking movement was recorded in tunnel segment until the final stage of the movement. In addition, the magnification of soil accelerations above the tunnel was found to be affected by tunnel depth in a number of analyses. For all frequency ranges, larger magnifications were observed with decreasing tunnel depth (see Figure 4).

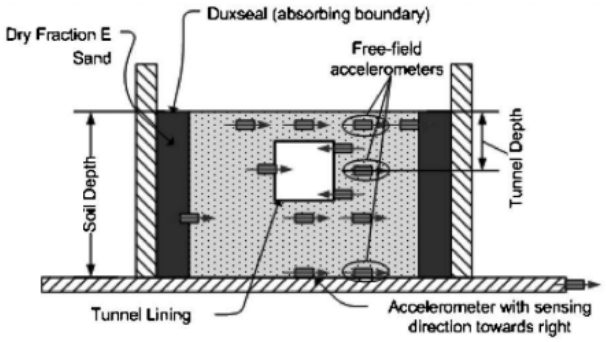

(a)

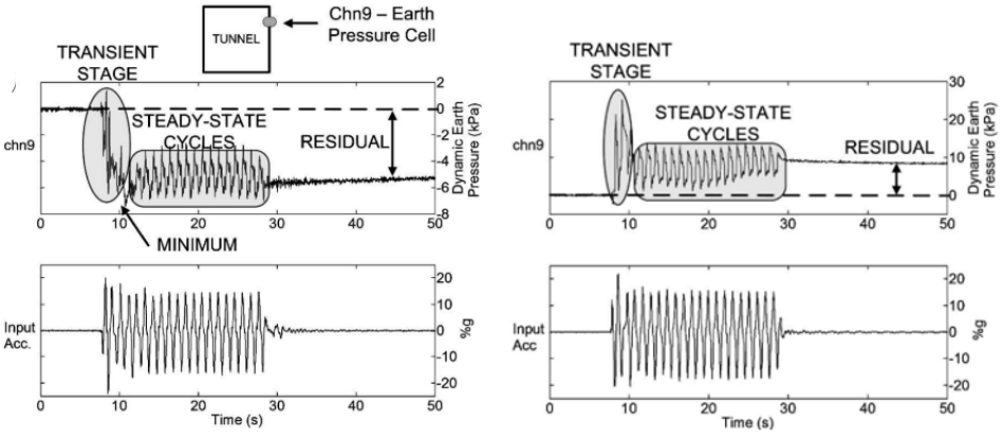

(b)

Figure 3. (a) Schematic representation of centrifuge tests, (b) Typical soil pressure time history from centrifuge tests (Çilingir and Madabhusi, 2011)

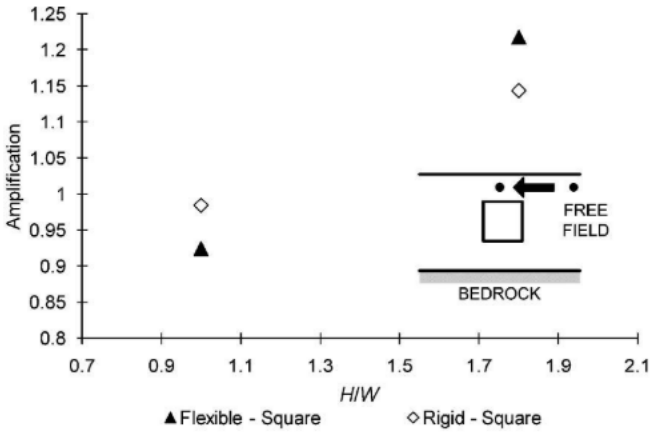

Figure 4. Amplification of peak acceleration for different depth/width ratios (H/W) (Çilingir and Madabhusi, 2011)

Earthquake-induced deformations of subterranean structures are mainly classified into three classes: axial, curvature, ovalling (for circular cross-sections) or racking (for rectangular cross-sections) (Owen and Scholl, 1981).

Axial and curvature deformations occur when the seismic wave of the earthquake is parallel to the structural section. Axial deformations develop as the tunnel is subjected to compressive and tensile effects during the cyclic loading of the earthquake, while curvature deformations can be positive or negative. The phenomenon of ovaling and racking deformations arises when seismic waves are oriented normal to the axial plane of a tunnel, thereby distorting the tunnel lining's cross-sectional shape (see Figure 5).

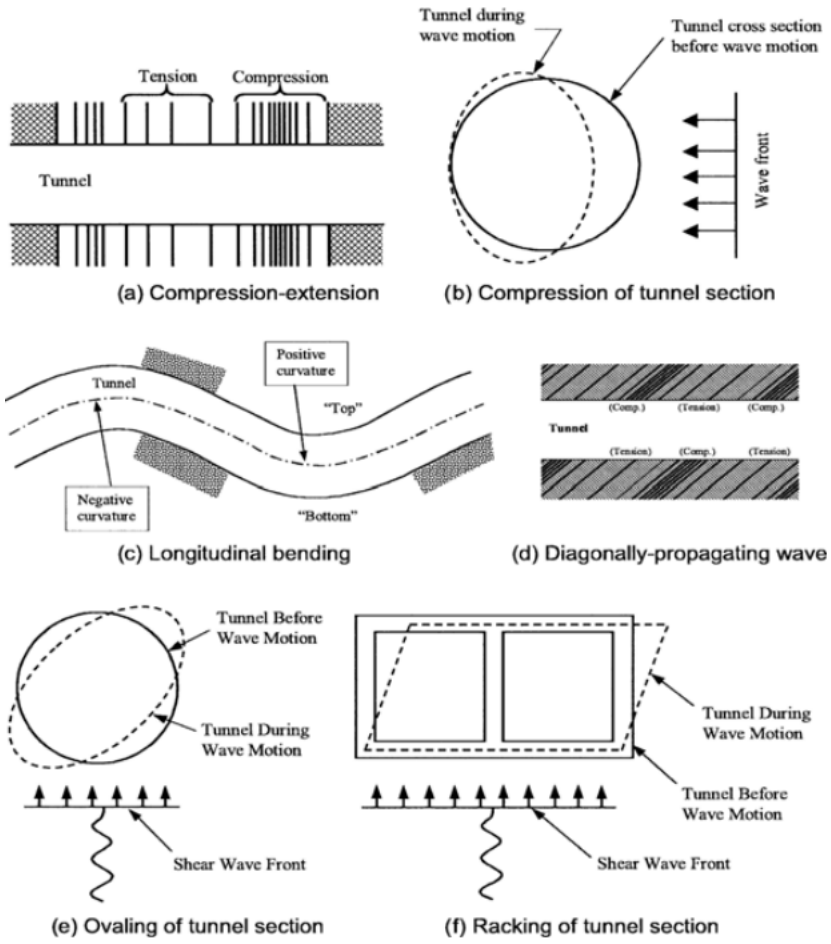

Figure 5. Earthquake-induced deformations of underground structures (a) axial deformations (b) curvature deformations (Owen and Scholl, 1981; Pitilakis and Tsinidis, 2010)

Axial and curvature deformations are generally less severe than oval or racking deformations. Therefore, they are not an initial design priority (Wang, 1993).

Penzien (2000) stated that in a homogeneous soil environment, a rectangular section of known width and height, with a length much greater than its width, will be subjected to the same deformations that the soil would undergo in the free-field condition during the expected seismic event, and that the most critical type of deformation that a fully buried structure will undergo during an earthquake is the racking deformation of the cross-section.

The deformation of underground structures is limited to the racking type, as the study deals with underground structures with rectangular cross-sections. The racking deformation is defined as the relative movement between the upper and lower levels of rectangular intersection (see Figure 6). The rack deformation represents the relative deformation between the upper and lower levels of the subway structure in the case of a rectangular cross section.

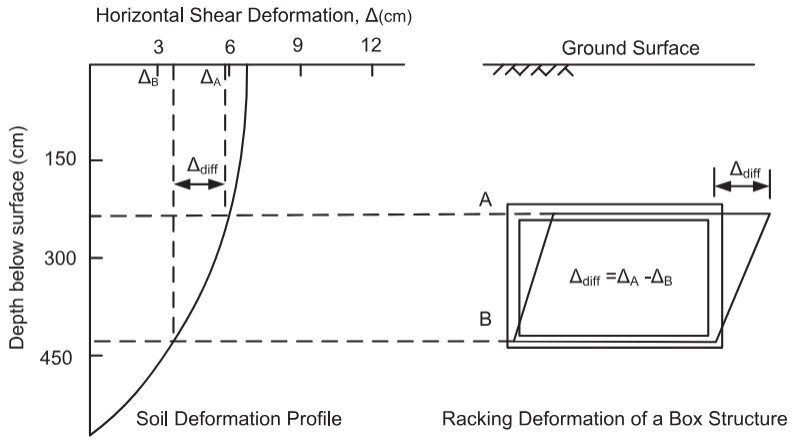

Figure 6. Rack deformation of a rectangular section (Wang, 2001; Lu and Hwang, 2017)

Strains and loads in a building during a seismic event are analysed on the basis of the theory of wave propagation in homogeneous, isotropic and elastic media. Using motion equations for the particles of the medium, the seismic wave propagating along x-plane is

expected to experience axial strain in the same direction ($\partial u/\partial x$) and curvature ($\partial^2 u/\partial x^2$) is expressed by Equation 2.1 and Equation 2.2 (Newmark, 1967).

$$\frac{\partial u}{\partial x} = -\frac{1}{c}\frac{\partial u}{\partial t} \tag{2.1}$$

$$\frac{\partial^2 u}{\partial x^2} = -\frac{1}{c^2}\frac{\partial^2 u}{\partial t^2} \tag{2.2}$$

It's here, $\partial u/\partial t$ and $\partial^2 u/\partial t^2$ represents velocity and acceleration of particles, respectively (t is time and c is the apparent wave propagation velocity).

Axial or longitudinal strain (ϵ_l) due to the P-wave, which causes the grain to move in the same direction as the waves, is described by Equation 2.3. Equation 2.4 describes the peak value of the axial or longitudinal strain (ϵ_{lm}) (Newmark, 1967).

$$\epsilon_l = \frac{\partial u_l}{\partial l} \tag{2.3}$$

$$\epsilon_{lm} = \pm\frac{V_p}{c_p} \tag{2.4}$$

Here, c_p is velocity of P-wave and V_p is velocity of peak grain.

Strains perpendicular to the direction of propagation are zero for P-waves. The shear strains are also zero.

Shear strain induced by the S-wave (γ_m)and curvature ($1/\rho_m$) is expressed by Equation 2.5 and Equation 2.6.

$$\gamma_m = \frac{V_s}{c_s} \tag{2.5}$$

$$\frac{1}{\rho_m} = \frac{a_s}{c_s^2} \tag{2.6}$$

Here, c_s is velocity of S wave, V_s is velocity of maximum particle and a_s is maximum acceleration of grains. For S-wave, the axial and normal strains are zero (Newmark, 1967).

The strains in directions of spreading of P- and S- waves are described by these equations. In reality, however, P and S waves typically propagate at a certain angle (φ) during the seismic event. This angle is usually unknown during seismic events, but its value at the most critical condition can be an estimate. The equations developed to estimate the most critical angles and maximum strain values are shown in Table 1. Racking deformations of underground facility due to shear deformations in the soil environment can be calculated using the shear strains in the Table 1 (John and Zahrah, 1987).

Table 1. Seismic shear wave and curvature (John and Zahrah, 1987; Hashash et al., 2001)

Wave type	Longitudinal strain	Normal strain	Shear strain	Curvature
P-wave	$\varepsilon_l = \frac{V_P}{C_P}\cos^2\phi$	$\varepsilon_n = \frac{V_P}{C_P}\sin^2\phi$	$\gamma = \frac{V_P}{C_P}\sin\phi\cos\phi$	$\frac{1}{\rho} = \frac{a_P}{C_P^2}\sin\phi\cos^2\phi$
	$\varepsilon_{lm} = \frac{V_P}{C_P}$ for $\phi = 0°$	$\varepsilon_{lm} = \frac{V_P}{C_P}$ for $\phi = 90°$	$\gamma_m = \frac{V_P}{2C_P}$ for $\phi = 45°$	$\frac{1}{\rho_{max}} = 0.385\frac{a_P}{C_P^2}$ for $\phi = 35°16'$
S-wave	$\varepsilon_l = \frac{V_S}{C_S}\sin\phi\cos\phi$	$\varepsilon_n = \frac{V_S}{C_S}\sin\phi\cos\phi$	$\gamma = \frac{V_S}{C_S}\cos^2\phi$	$K = \frac{a_S}{C_S^2}\cos^3\phi$
	$\varepsilon_{lm} = \frac{V_S}{2C_S}$ for $\phi = 45°$	$\varepsilon_{nm} = \frac{V_S}{2C_S}$ for $\phi = 45°$	$\gamma_m = \frac{V_S}{C_S}$ for $\phi = 0°$	$K_m = \frac{a_S}{C_S^2}$ for $\phi = 0°$
Rayleigh wave Compressional component	$\varepsilon_l = \frac{V_{RP}}{C_R}\cos^2\phi$	$\varepsilon_n = \frac{V_{RP}}{C_R}\sin^2\phi$	$\gamma = \frac{V_{RP}}{C_R}\sin\phi\cos\phi$	$K = \frac{a_{RP}}{C_R^2}\sin\phi\cos^2\phi$
	$\varepsilon_{lm} = \frac{V_{RP}}{C_R}$ for $\phi = 0°$	$\varepsilon_{nm} = \frac{V_{RP}}{C_R}$ for $\phi = 90°$	$\gamma_m = \frac{V_P}{2C_R}$ for $\phi = 45°$	$K_m = 0.385\frac{a_{RP}}{C_R^2}$ for $\phi = 35°16'$
Shear component		$\varepsilon_n = \frac{V_{RS}}{C_R}\sin\phi$	$\gamma = \frac{V_{RP}}{C_R}\cos\phi$	$K = \frac{a_{RS}}{C_R^2}\cos^2\phi$
		$\varepsilon_{nm} = \frac{V_{RS}}{C_R}$ for $\phi = 90°$	$\gamma_m = \frac{V_{RS}}{C_R}$ for $\phi = 0°$	$K_m = \frac{a_{RS}}{C_R^2}$ for $\phi = 0°$

The Poisson's ratio and dynamic modulus of a soil deposit can be computed from measured P- and S-wave propagation velocities in an elastic medium: $v_m = \frac{1}{2}\frac{(C_p/C_s)^2 - 2}{(C_p/C_s)^2 - 1}$ or $C_P = \sqrt{\frac{2(1-v_m)}{(1-v_m)}}C_S$; $E_m = \rho C_P^2\frac{(1+v_m)(1-2v_m)}{(1-v_m)}$; and $G_m = \rho C_S^2$, respectively.

Subsurface structures with a rectangular cross-section buried in the ground are less capable of transferring loads than those with a circular cross-section. This is due to the bending effect. Under load, underground structures with a circular cross section are subject to compression, while those with a rectangular cross section are subject to bending. Therefore, the walls and slabs of a rectangular underground structure are typically thicker and therefore stiffer than those of a circular cross-section. The increased stiffness of a rectangular structure results in less strain. This makes the design of rectangular underground structures relying on free-field strains overly conservative. (Kwang and Lysmer, 1981).

The free field deformations of the soil induced by the seismic wave are modified by the structure. Similarly, the free field vibration of the structure is constrained by the ground (Wang, 1993). In structure-ground interaction problems, at a sufficiently large distance from the structure, the ground deforms freely, similar to free field conditions. However, in the vicinity of the structure, motion is modified by the existence of the facility. By limiting the reduction in the shear moduli of soil with which they interact, rigid structures reduce soil deformation. However, if the structure is sufficiently flexible, the soil may be subjected to greater shear stresses than in the free state and the shear modulus may be significantly reduced. In this case, the soil may deform more than in the free state (Huo et al., 2005).

Huo et al. (2005) described this behavior with analyses for the Daikai station, as shown in Figure 7. In the regions close to building (at a distance equal to the structural height), the shear modulus reduction was suppressed by the structure. And at a far enough distance, the soil experienced a large shear modulus reduction, similar to free field conditions.

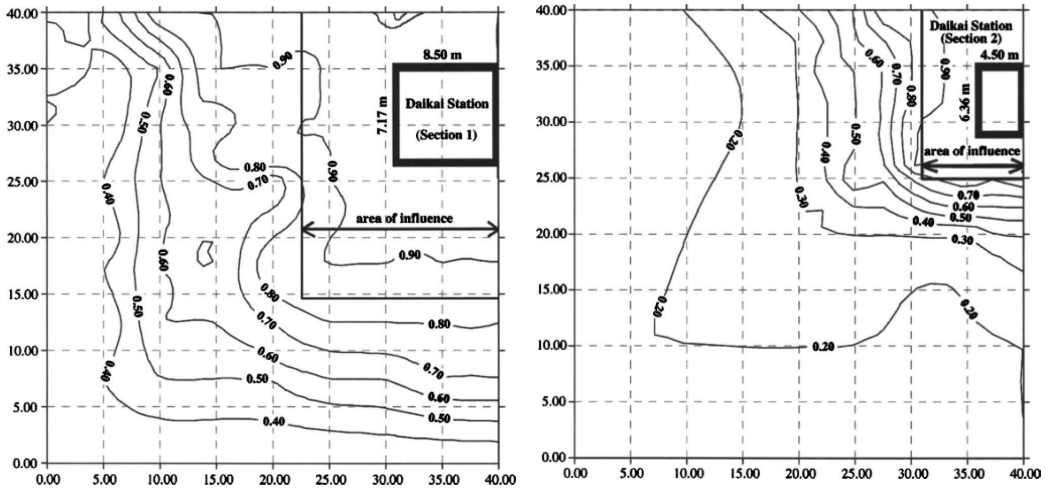

(a) (b)

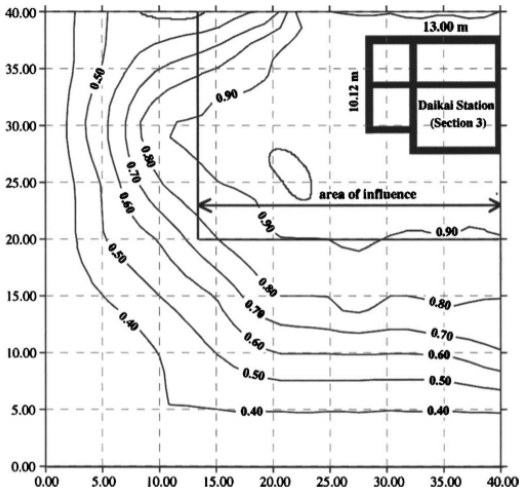

(c)

Figure 7. Degradation plots of shear modulus (G/G_{max}) in vicinity of the underground structure (a) Section 1 of Daikai metro station (b) Section 2 of Daikai metro station (c) Section 3 of Daikai metro station (Axes are distance in meters and the curves represent the shear modulus reduction)

The interaction between the soil and the facility is governed by several parameters: the stiffness difference between facility and ground, structural parameters, earthquake excitation characteristics and depth of burial of underground structure. The stiffness difference between facility and ground is most important of these parameters. The relative stiffness difference is known in the literature as the flexibility ratio. For a rectangular underground construction, the flexibility ratio reflects difference in flexural stiffness

between soil medium and construction. Under simple shear conditions, the flexibility ratio changes the lateral racking stiffness of the structure (Wang, 1993).

The simple shear of a ground particle in a base case (τ), the shear strain (γ) and the shear stresses are given in Equation 2.7 (Wang, 1993).

$$\gamma_{soil} = \frac{\Delta}{H} = \frac{\tau}{G} \tag{2.7}$$

Here, G is the shear modulus of soil, Δ is the shear deflection over structural height and h is structural height (see Figure 8 for simplified representation)

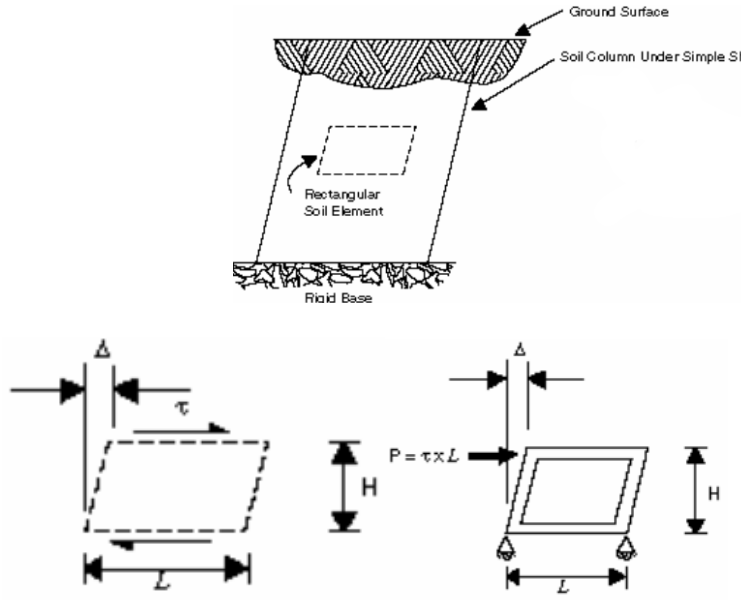

(a) (b)

Figure 8 Shear deformation of underground structures in the case of simple shear (a) free-field soil medium (b) rectangular frame (Wang, 1993)

The shear stress acting on the soil (τ) will also act on the structure. This stress is expressed as a concentrated force applied to the construction. This stress may be described as a concentrated load on the structure. If it is considered that the concentrated force is acting along the width (L) of the structure, then $P = \tau \times L$ is taken into consideration. Equation 2.8 defines the shear strain of the structure under this load. (Wang, 1993).

$$\gamma_{structure} = \frac{\Delta}{H} = \frac{\tau L}{HS_1} \quad (2.8)$$

Here, S_1 is the force required for the structure to make unit racking deformation.

Equation 2.9 shows the flexibility ratio (F), which is defined as the ratio of Equation 2.7 and Equation 2.8.

$$F = \frac{GL}{S_1 H} \quad (2.9)$$

The flexibility ratio of a rectangular structure is given by Equation 2.10, depending on the moments of inertia of the roof, floor and side walls (Wang, 1993; Hashash et al., 2001).

$$F = \frac{G}{24}\left(\frac{H^2 L}{EI_W} + \frac{HL^2}{EI_R}\right) \quad (2.10)$$

Here, I_R is the same moment of inertia of the ceiling slab and the invert slab, I_W is moment of inertia of sidewalls and E is elasticity moduli of structural frame.

Equation 2.11 can be used if the ceiling and invert slabs of the structure have different moments of inertia (Wang, 1993; Hashash et al., 2001).

$$F = \frac{G}{12}\left(\frac{HW^2}{EI_R}\psi\right) \quad (2.11)$$

Here,

$$\psi = \frac{(1+a_2)(a_1+3a_2)+(a_1+a_2)(3a_2+1)}{(1+a_1+6a_2)^2} \tag{2.12}$$

$$a_1 = \left(\frac{I_R}{I_I}\right) \tag{2.13}$$

$$a_2 = \left(\frac{I_R}{I_w}\right)\left(\frac{H}{W}\right) \tag{2.14}$$

Also, I_R is the moment of inertia of the ceiling slab and I_W is the moment of inertia of the invert slab.

Wang (1993) proposed the relationship between the flexibility ratio and normalized structure deflections as shown in Figure 8. According to this relationship, in the case of a perfectly rigid structure, where the flexibility ratio is close to zero, the structure does not show any deformation independent of the free field soil deformations. For an axis ratio greater than 1.0, the structure is more flexible than the soil and rack deformation of building is greater than free field deformations of the soil.

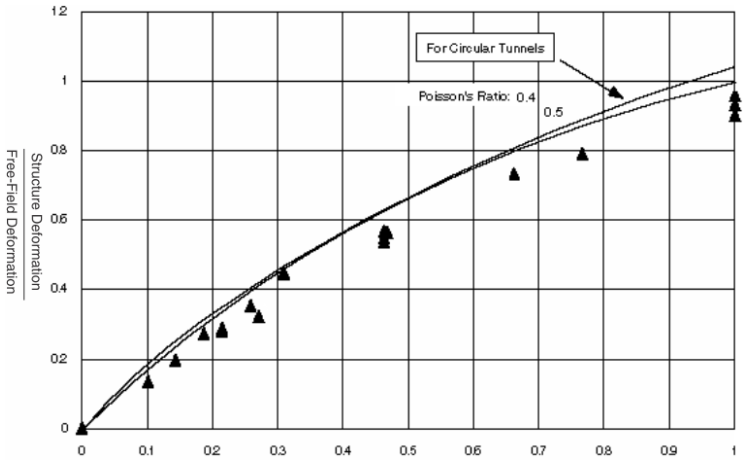

Figure 8. The relationship between the flexibility ratio and normalized structure deflections for rectangular tunnels (Filled triangles represent rectangular tunnels and solid lines represent circular tunnels) (Wang, 1993)

The racking coefficient (R) characterizes racking deformations of rectangular underground facility due to earthquake accelerations. The racking coefficient is the ratio of lateral rack deformations of building to the lateral shear deformations in free-field conditions and can also be referred to as the normalized structural displacement. (see Equation 2.15; Wang, 1993).

$$R = \frac{\Delta_{structure}}{\Delta_{free-field}} = \frac{\left(\frac{\Delta structure}{H}\right)}{\left(\frac{\Delta free-field}{H}\right)} = \frac{\gamma_{structure}}{\gamma_{free-field}} \quad (2.15)$$

Here, $\gamma_{structure}$ is the shear strain of the structure, $\gamma_{free-field}$ is shear strain in free-field conditions.

The shear stress acting on the structure can be calculated using Equation 2.16 (Pitilakis and Tsibidis, 2010).

$$\tau_{structure} = G \times \gamma_{structure} \quad (2.16)$$

Wang (1993) stated that the racking coefficient increases with the flexibility ratio (see Figure 9). In addition, as a result of analyzing scenarios where the flexibility ratio remains constant but the structure has different buried depths, it is found that the racking coefficient decreases with decreasing buried depth in conditions where the buried depth of the structure is equal to or less than the height of the structure ("shallow buried" condition). The relationship between the racking coefficient and the burial depth in the case where the flexibility ratio remains constant is described as shown in Figure 10.

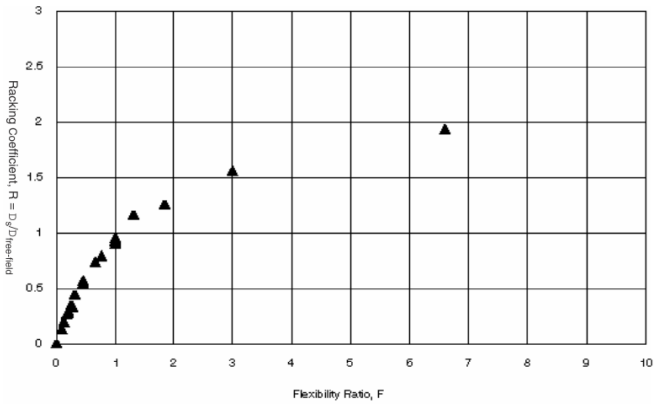

Figure 9. The relationship between the flexibility ratio and racking coefficients for rectangular tunnels (Wang, 1993)

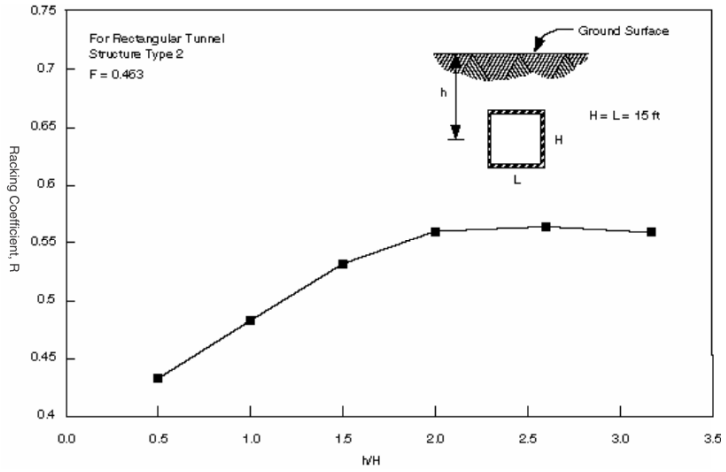

Figure 10. The relationship between the racking coefficient and the burial depth (Wang, 1993)

Xu et al. (2019) stated that the vertical earthquake component had no influence on seismic horizontal deformation of the underground facility in their analyses performed with a series of equivalent linear models based on the Daikai station case (see Figure 11). However, the vertical earthquake load has an effect on the collapse mechanism of the structure by increasing the internal forces in the structural elements.

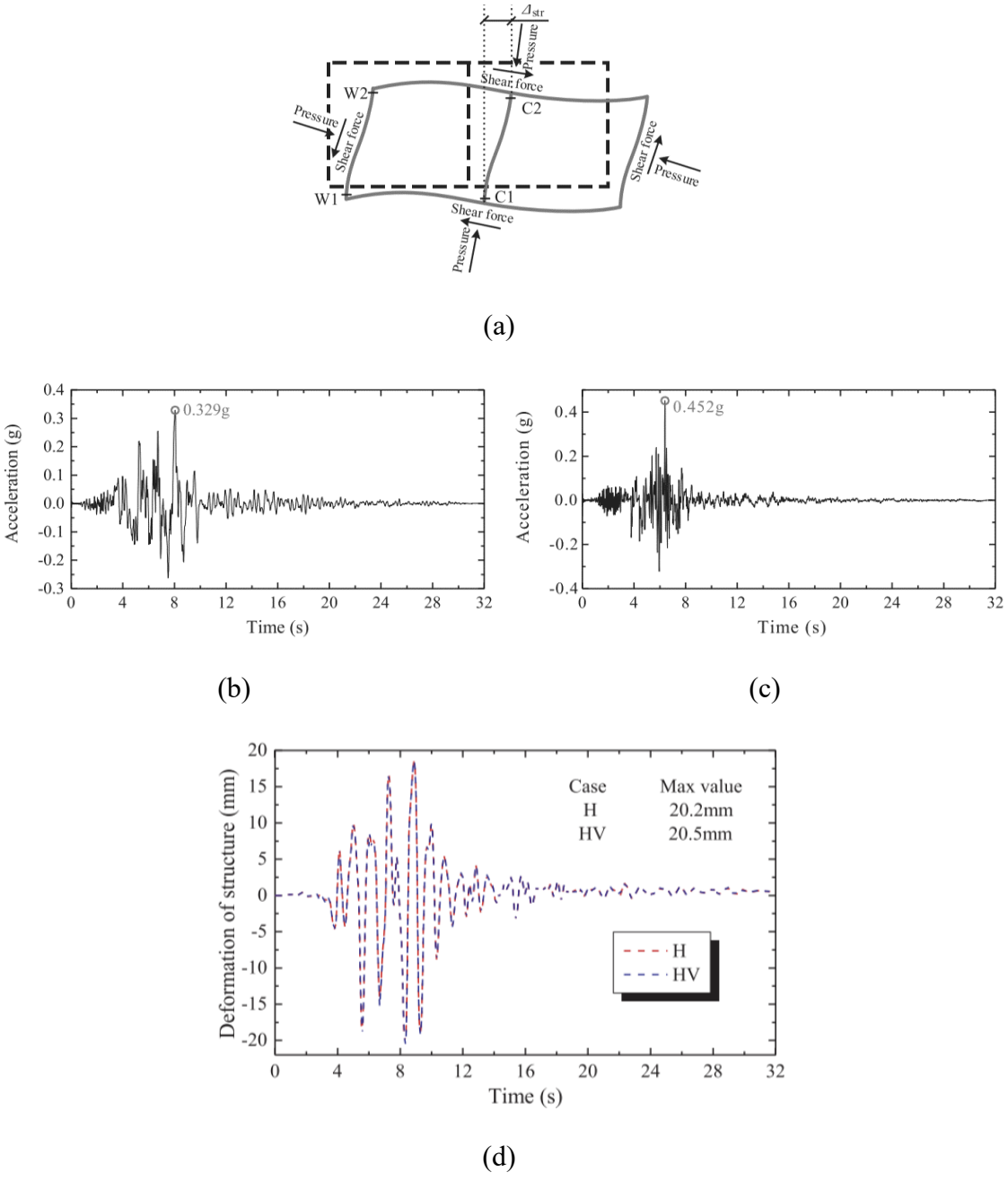

Figure 11. Deformation analyses of Daikai station under different earthquake loads (a) body diagram for Daikai metro station (b) Horizontal component of earthquake records at the Kobe University station (c) Vertical component of earthquake records at the Kobe University station (d) Deformations of the structure under horizontal and vertical earthquake loads (Xu et al., 2019)

In addition, Xu et al. (2019) stated that structural internal forces are not a parameter that affects the horizontal seismic deformation of the structure, since the seismic deformation profile of structures having different structural densities is similar. But the density of the

soil surrounding the structure can greatly affect the response. No significant change in the values of the soil pressures acting on the structure was observed as a result of changing the friction coefficient, which represents the frictional relationship between soil and underground facility. However, as coefficient of friction increases, soil shear forces around the structure are found to increase gradually. Since influence of underground structures on the earthquake response of surface soils is not investigated in terms of subsidence in this thesis, vertical earthquake effects are not prioritized as a special parameter.

2.3. Pseudo-Static Methods

The basic stages of seismic analysis and design of underground structures can be summarized as determining the seismic hazard and design criteria, determining the ground response induced by the seismic event and determining structural seismic response (Pitilakis and Tsinidis, 2010). In soil structure interaction analyses, where response of building is determined, analytical, pseudo-static or dynamic analysis methods are applicable (Hashash, 2010).

Although analytical methods can provide good parametric predictions, their application is limited because they do not consider the soil-structure-earthquake interaction. Dynamic time-history analyses, on the other hand, require non-linear material and interaction parameters, complex seismic inputs and precise boundary conditions due to the modelling of complex structure-soil interaction. Especially in cases with multiple seismic inputs, the complexity of these inputs and parameters becomes an operational burden. In these cases, pseudo-static analysis is an effective option (Wang, 2001; Huo, 2005; Hashash, 2010; Yang et al., 2023).

In pseudostatic analysis, earthquake motion is represented as equivalent to free field ground deformations. These seismic deformations, which will occur far enough away from the structure, are calculated using free-field ground response analyses. These calculated free field deformations are seismic strains that will occur in the ground far enough away from the structure during an earthquake. At a sufficient distance from the structure, the ground returns to free field conditions (Pitilakis and Tsinidis, 2010). In

pseudo-static analyses, the soil-structure interaction is simplified as frame system in ground environment subjected to shear in the vertical and horizontal planes. Due to this simplification, earthquake induced soil-structure interactions are ignored (Hashash, 2010).

Ground response analyses are performed to assess the effect of the seismic wave propagating through ground as a first step in pseudostatic analyses. Non-linear soil behavior under repeated loading is simulated using one-dimensional wave propagation software (Hashash, 2010; Pitilakis and Tsinidis, 2010).

One-dimensional ground response analysis software (e.g. DEEPSOIL, SHAKE, etc.) is used to determine the maximum deformation profile that will occur in the soil environment where the structure is situated. Soils tend to lose their shear stiffness rapidly under large and repeated shear loads of the earthquake in free field conditions where there is no structure. The decrease in shear stiffness occurs in parallel with the increase in shear deformation. When subjected to cyclic earthquake loading, the soil exhibits hysteretic behavior at the moments of load removal. Hysteretic behavior is generally frequency independent and depends on the damping properties of the material. Accurate prediction of this non-linear behavior of the soil is possible using material models (Huo et al., 2005).

Then, in the two-dimensional numerical analysis step, the structure is simplified as a frame in the ground. The box frame is modelled according to the axial and bending stiffness of structure. The shear resistance of ground is calculated from strain-compatible shear wave velocities obtained in the previous stage. The seismic force is applied by imposing deformations of free field on structure in form of lateral deformations. This simplification reflects seismic shear deformations that surrounding soil would actually transmit to the structure. The racking deformations that the structure will undergo under these lateral forces are then calculated using two-dimensional analysis software (e.g. Plaxis, etc.) (Hashash, 2010).

Figure 12 summarizes the steps of the pseudo-static analysis method (Monsees and Merritt, 1988; Wang, 1993).

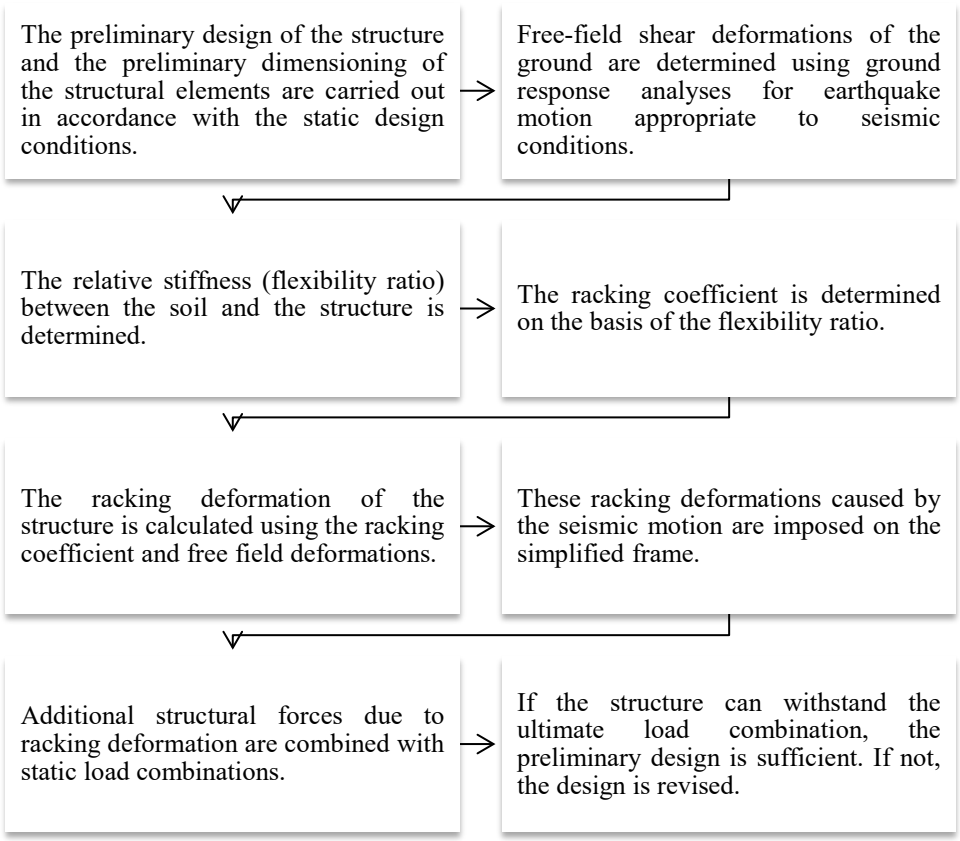

Figure 12. The steps of the pseudo-static analysis method (Monsees and Merritt, 1988; Wang, 1993)

A cost-effective approach is offered by pseudo-static analysis. However, the results of the analysis can be significantly altered by steps such as modelling heterogeneous soil structure or defining model boundaries. For example, if the model boundaries are set too far away from building, the vast weight of soil between facility and model boundaries may absorb some of the deformations. Conversely, if the boundaries are set too close to the structure, the mechanism by which the structure and soil interact may not be fully assessed (Pitilakis and Tsinidis, 2010).

Hashash et al (2010) carried out pseudo-static and dynamic soil-structure interaction analyses using 14 different ground motions to determine the racking deformations of a box section underground structure buried in soft and soft soils. Equivalent linear and nonlinear methods are used to compare one-dimensional soil response analyses, which

form the basis of two-dimensional soil-structure interaction analyses. The results of the numerical analyses show that the pseudo-static analysis method will provide an accurate evaluation with less effort compared to the dynamic analysis method in stiff soils. However, as the stiffness of the soil decreases, the pseudo-static analysis can give more conservative results than the dynamic analysis (see Figure 13).

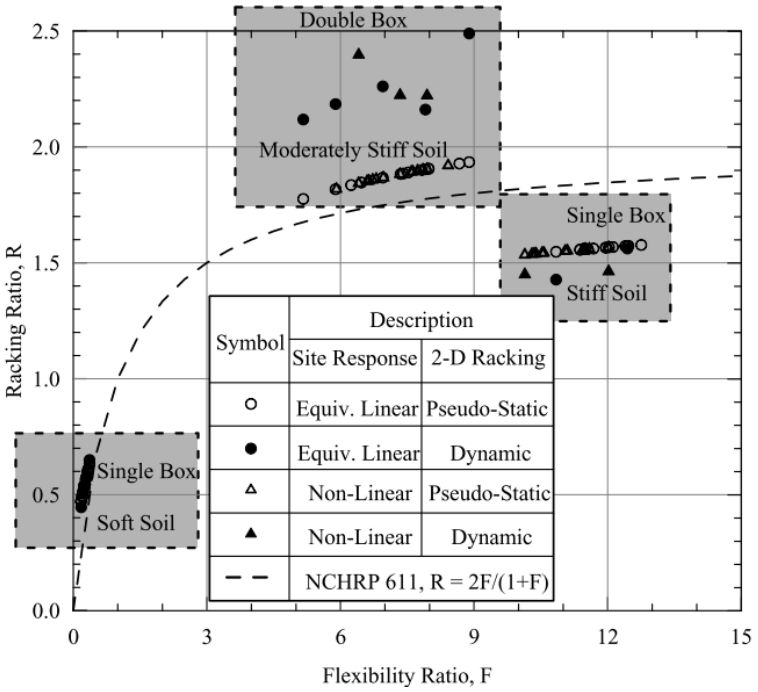

Figure 13. Pseudo-static and dynamic analysis of the correlation between racking coefficient and flexibility ratio (Hashash et al., 2010)

Huo et al (2005) investigated collapse mechanism of Daikai subway station, emphasizing on the load transmit system between sub-surface facility and the adjacent ground. Two main parameters were found to govern load transmit mechanism between sub-surface facility and adjacent ground: the relative rigidity difference between building and soil, and the friction behavior of boundary layer. As the rigid underground structure is dominated by the surrounding soil, it exhibits relatively small deformation and decrease in shear stiffness of soil under repeated loading is limited, preventing further deformation of the soil. This means that the deformation required of the structure is reduced. However, more shear forces may be transferred to the structure at interface of structure-soil.

Another important component of structure-soil interaction is interfacial friction. Loads and/or deformations transmitted from soil to structure are affected by nature of the friction at the interface. The effect of friction is to cause the loads and deformations that act on the structure to be different from the loads and deformations that develop in the soil under free field conditions. The frictional characteristics at the interaction interface must be properly considered to realistically predict earthquake behavior of an underground facility.

Huo et al. (2005) carried out analyses with different friction coefficients highlight the impact of friction properties on deformation of an sub-surface structure (see Figure 14). Despite the different friction coefficients, it can be seen that the maximum deformation occurs in the first few cycles of earthquake motion, the maximum deformation occurs simultaneously as the maximum acceleration of earthquake, and the deformations decrease with time (in the absence of failure). However, in the full slip condition, where the friction coefficient is zero, the central deformation is symmetrical with relatively small permanent deformations. In the other two cases, the permanent deformations are much larger in the first few cycles of the earthquake. This difference in behaviour is caused by the deformations in full shear conditions being induced only by the normal stress. In presence of friction, deformations are induced by both normal and shear stresses. On other hand, largest deformations occurred in the friction coefficient (μ) is 0.4 condition.

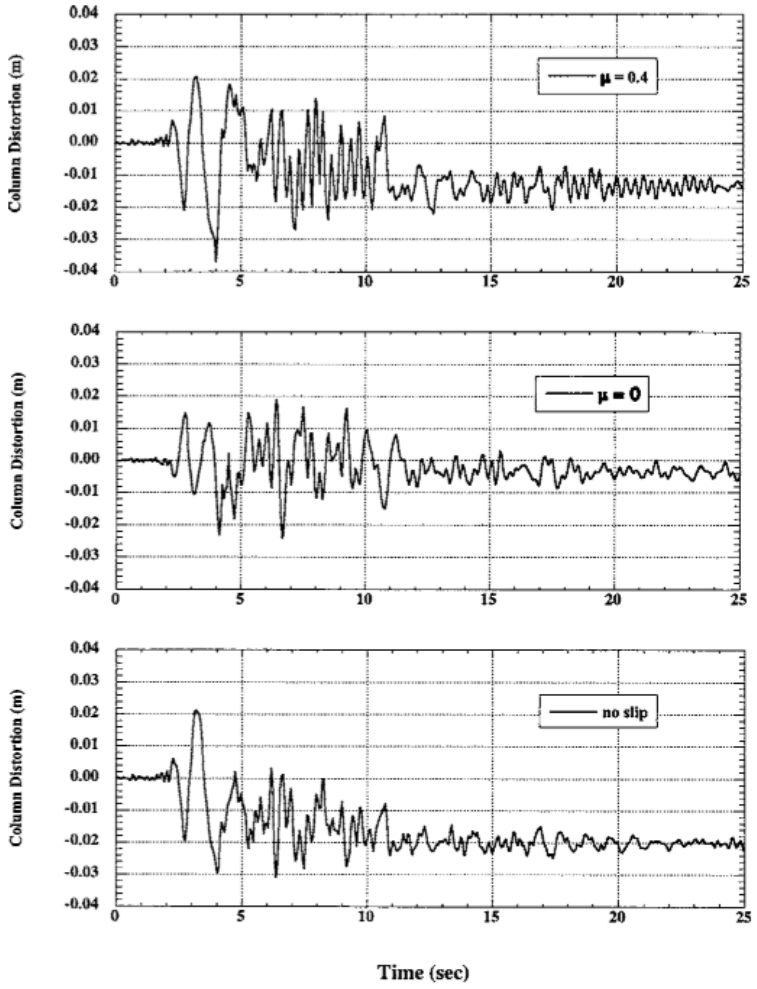

Figure 14. Deformation of the Daikai station for different scenarios of interface friction (Huo et al., 2005)

The friction condition $\mu = 0.4$, which represents the most critical scenario of soil-structure interaction, has been used in the analyses of this thesis to create a realistic load transfer mechanism. This value allows a realistic assessment of the soil phenomenon, whose behavior is limited by the presence of the structure with increasing coefficient of friction.

2.4. Effects of Surface Soil and Overburden Depth on Seismic Behavior of Underground Structure

Sharma and Judd (1991) compared the earthquake performance of 191 cases of underground structures and reported that structures with a surface soil thickness of less than 50 m suffered severe damage and structures with a surface soil thickness of more than 300 m suffered almost no damage.

Unutmaz (2014) performed analyses based on the three-dimensional finite difference method to evaluate the cyclic behavior of circular tunnels and the liquefaction potential of the soils surrounding these tunnels. In the analyses performed for tunnel scenarios with different geometric parameters, it was found that the most critical parameter for liquefaction risk of surrounding soil is tunnel depth. Relatively shallow tunnels are more susceptible to liquefaction (see Figure 15 and Figure 16).

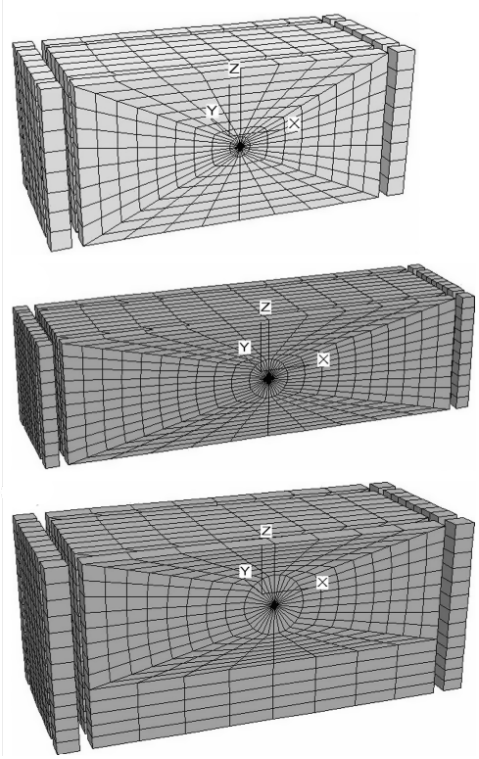

Figure 15. Finite difference model meshes (D is tunnel diameter and z is tunnel depth, from top to bottom; D=4 m and z=15 m, D=10 m and z=15 m, D=10 m and z=10 m, D=10 m and z=10 m) (Unutmaz, 2014)

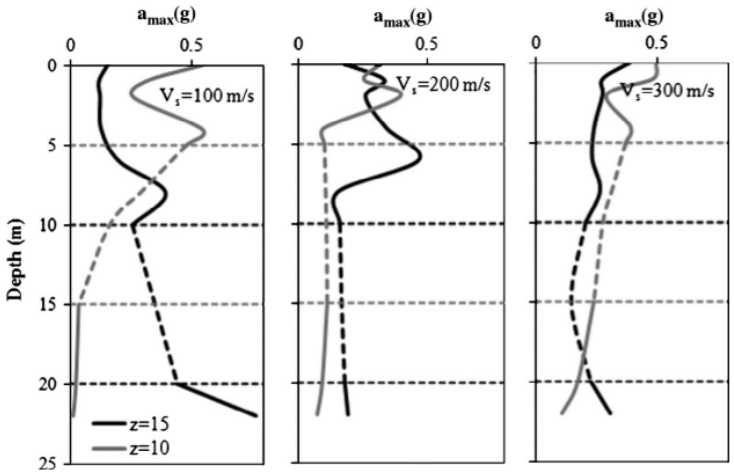

Figure 16. Comparison of maximum accelerations for different tunnel depths when the tunnel diameter (D) is 10 m (Unutmaz, 2014)

Andreotti and Lai (2015) investigated the effect of stresses transferred from the surface soil on deep tunnels in rock media, by performing several dynamic analyses under parametrically varying overburden conditions. Tunnels with 100 m, 350 m and 500 m overburden were analyzed under seismic events of different intensities. It was found that the loads acting on the tunnel lining increase by a factor of about 5 with increasing overburden depth (100 m and 500 m overburden cases) (see Figure 17). As a result of this load increase, the seismic response of the deeper underground structure changes from ductile to brittle.

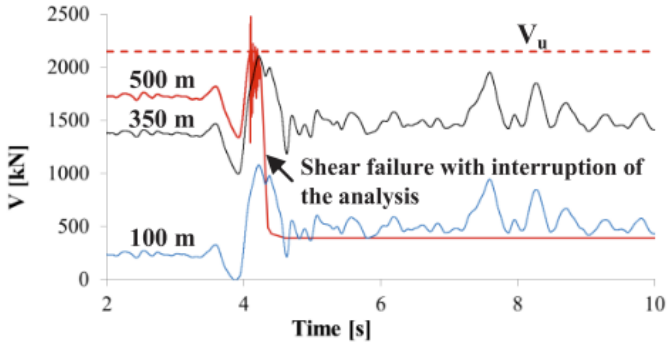

Figure 17. Time histories of the shear force of underground structures embedded in rock with different overburden depth (Andreotti and Lai, 2015)

Tsinidis (2020) analysed earthquake reaction characteristics of rectangular section tunnels buried in soils with relativelty little strength with different relative stiffness and interface properties for different shape, size and burial depth conditions and for different soil-earthquake conditions. One of the analysis models used is shown in Figure 18. The relationship between elasticity ratios (F) and racking coefficients (R) of rectangular section tunnels with different burial depths is defined as shown in the figure. It can be seen that the variation in depth and shape parameters has a significant effect on the deformation of the tunnel section under free field conditions and the normalised mean rotation (θ); the tunnel section with the same structural characteristics is subjected to more stress under relatively shallow conditions.

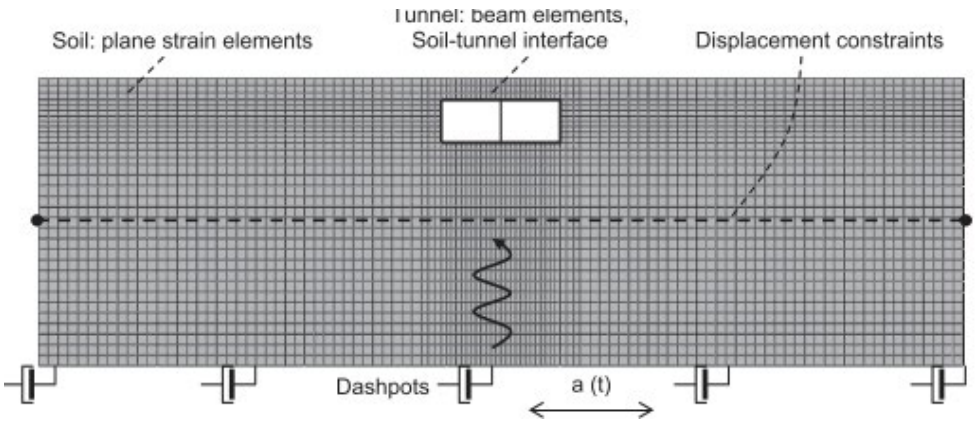

(a)

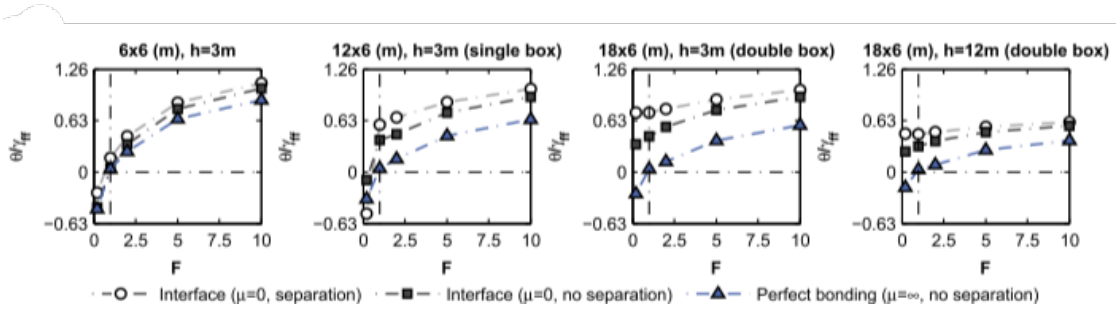

(b)

Figure 18. Overburden effect on seismic behavior of rectangular tunnel a) numerical model, b) relationship between normalized average rotation of lining and flexibility ratio (Tsinidis, 2020)

Focusing on subway stations, Li and Chen (2020) investigated impact of overburden depth on earthquake reaction of underground structures. As a result of three-dimensional nonlinear finite element analyses performed for this purpose, it was found that the overburden depth changes the structural resonant frequency and significantly affects response of underground structure (see Figure 19 for analysis models). The complex effect of the surface soil effect, which increases with depth and changes the resonant frequency of the structure, the axial compression ratios of the structural columns and the soil-structure interface characteristics, is shown in Figure 20.

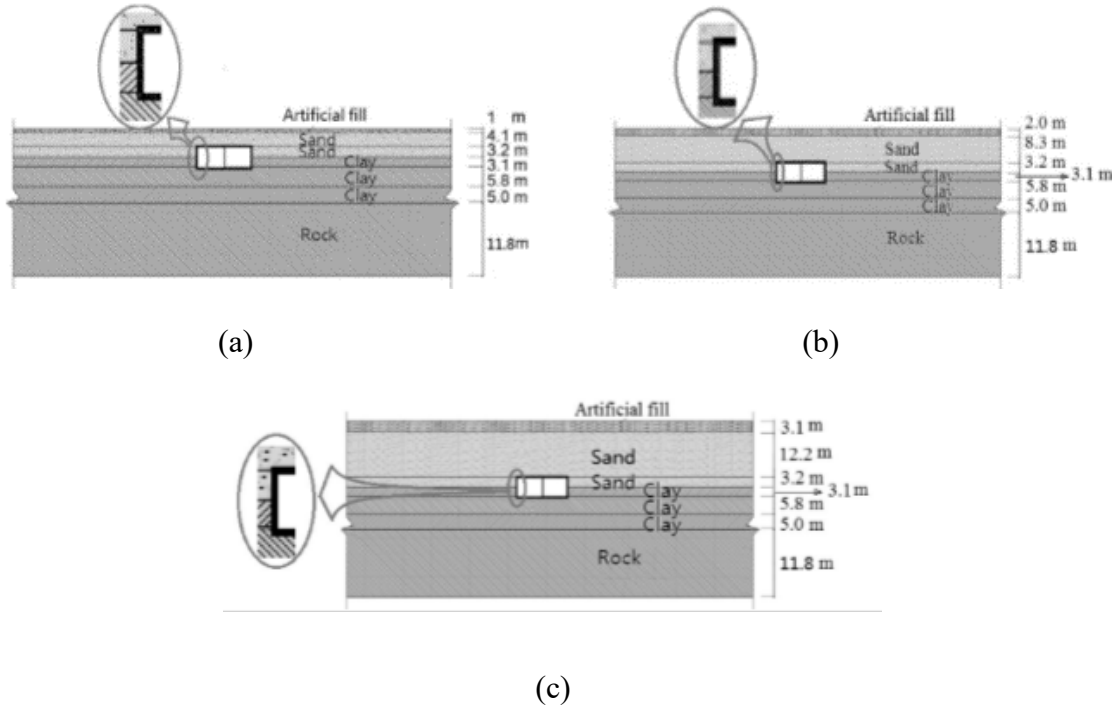

Figure 19. Metro station models with different burial depths a) burial depth 4.8 m, b) burial depth 10 m, c) burial depth 15 m (Li and Chen, 2020)

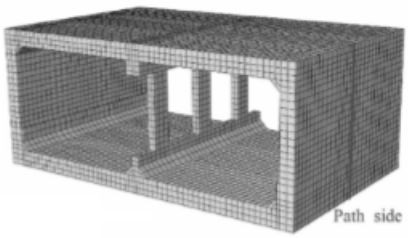

(a)

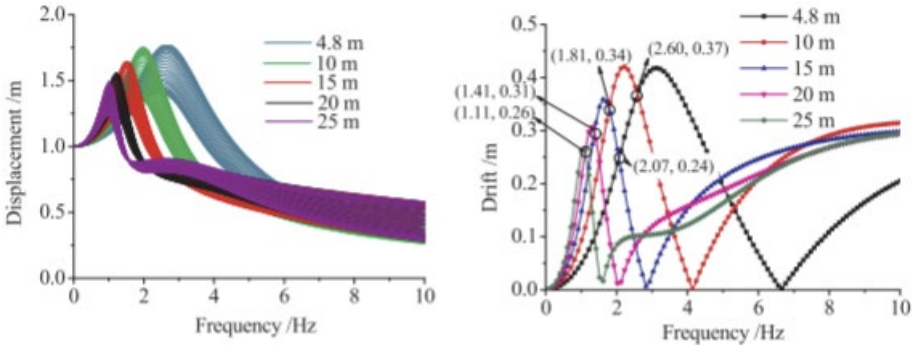

(b) (c)

Figure 20. Influence of overburden depth on earthquake reaction of underground metro station a) definition of path side, b) nodal displacement responses along path side, c) structural drift responses along path side (Li and Chen, 2020)

Golshani and Rezaeibadashiani (2020) performed numerical analyses for a shallow tunnel in order to express the parameters impacting the earthquake reaction of cut-and-cover tunnels. As a result of analyses performed with model shown in Figure 21, it was found that axial forces and bending moments acting on walls and slabs of underground structure increased with increasing depth for tunnels with 2 m, 4 m and 6 m overburden thickness. Although the maximum acceleration of the seismic event is reduced in the deeper buried tunnel, it is subjected to relatively higher forces than in the surface buried case (see Figure 21).

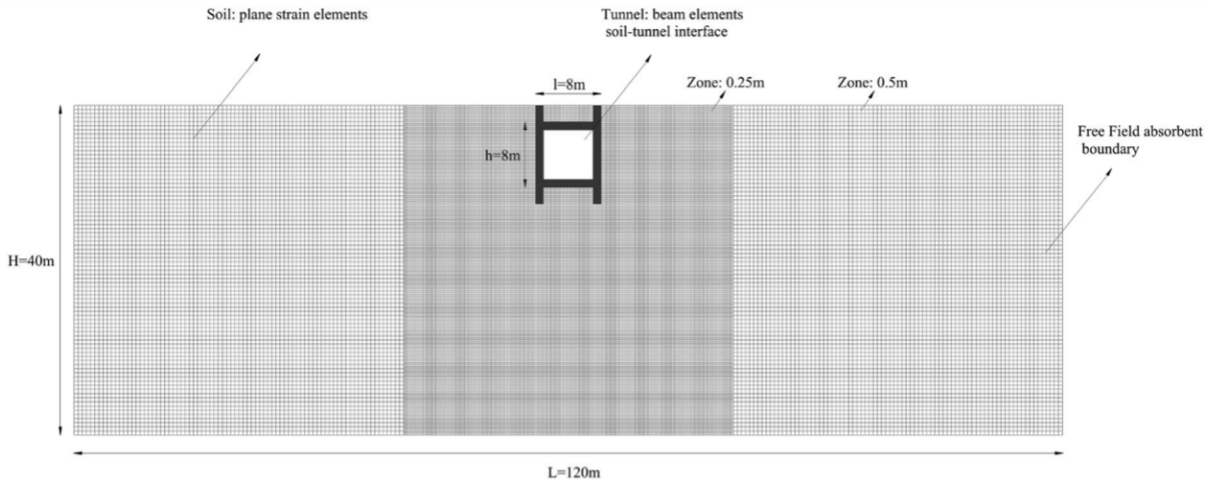

(a)

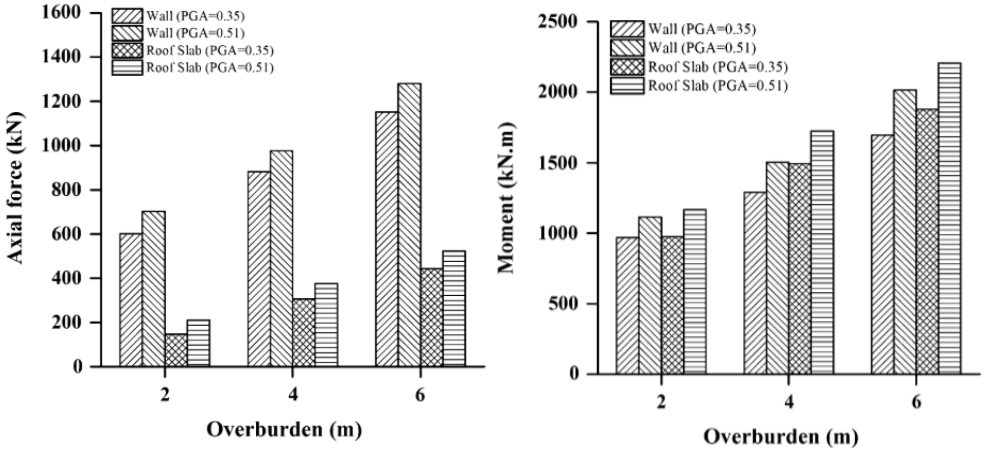

(b) (c)

Figure 21. Overburden effect on seismic behavior of cut and cuver tunnel a) numerical model, b) effect on maximum dynamic axial force of tunnel slabs and walls, c) effect on maximum dynamic bending moment of tunnel slabs and walls (Golshani and Rezaeibadashiani, 2020)

2.5. Overview

On the basis of the existing literature, the following conclusions can be reached:

- Pseudo-static analyses provide a cost-effective approach for deformation capacity-oriented analyses in earthquake design of sub-surface facilities. However, for this method, parameters such as model boundaries can directly affect the analysis results. It can also lead to an overly conservative design in soft soils.

- The main parameters affecting the seismic reaction of underground facilities are flexibility ratio and racking coefficient. These parameters are used to evaluate ability of underground structure to withstand a seismic event.

- By changing the flexibility ratio and racking coefficient of the structure, the nature of soil-structure friction, structural characteristics of underground structure and earthquake motion characteristics significantly influence seismic behavior.

However, there has been a lack of understanding of the load transfer mechanism between surface ground and the underground facility in behavior of structure modified by the surrounding soil.

The objective of this thesis is the evaluation of the effects of surface soil properties on the seismic behaviour of underground structures with rectangular cross section by means of pseudo-static analysis.

3. METHODOLOGY

3.1. Introduction

This thesis focuses on impact of surface soil properties on seismic behavior of rectangular underground structures. For this purpose, the rectangular sub-surface structure is analyzed by using pseudo-static method for different surface soil scenarios.

As stated in the preceding section, firstly, response of soil to seismic event in free field conditions without structure was determined by soil response analyses using DEEPSOIL software. Then, rack deformations of structural components under these forces were calculated by imposing free-field deformations on two-dimensional model boundaries far enough away from the structure. PLAXIS software was used for the two-dimensional analyses.

Surface soil scenarios with varying shear wave velocities, shear strengths and plasticity indices were created to determine the impact of surface soil on earthquake response of structure. The ground conditions surrounding the underground structure were kept constant despite the change in surface soil. Thus, impact of the ground at surface can be clearly described. A selected strong earthquake event was used in all analyses.

3.2. Numerical Modelling

The soil properties, structural parameters and earthquake motion parameters that form the basis of the study are described in detail in this section.

3.2.1. Soil profiles

The soil profiles are assumed to consist of uniform clay units. The clay units extend to a depth of 30 m and consist of 3 distinct layers. Accordingly, 0.00-5.00 m depths were defined as Clay 1 unit (Surface Soil), 5.00-12.00 m depths as Clay 2 unit (Surrounding Soil) and >12.00 m depths as Clay 3 unit (Base Soil) (see Table 2 and Table 3 for geotechnical parameters of the soil units). In this way, the changing seismic response of

the station structure buried 5 m below the surface, with the surrounding and base soils remaining constant despite the changing surface soil properties, is clearly demonstrated (see Figure 22 for schematic representation).

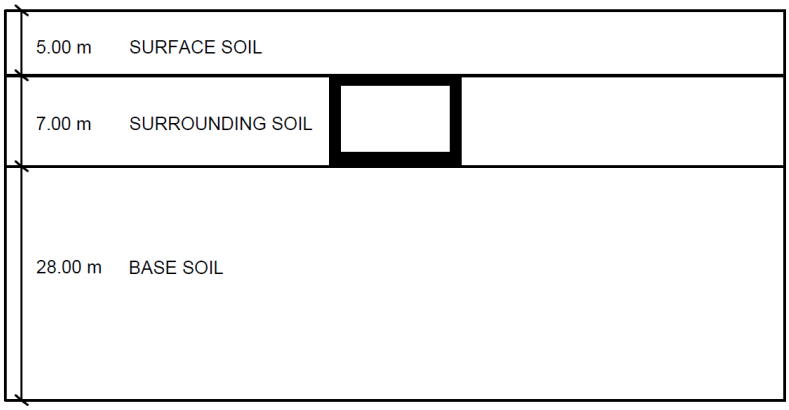

Figure 22. Schematic views of soil layers

Table 2. Geotechnical parameters of surrounding and base soil

Soil Layer	**Surrounding Soil**	**Base Soil**
Soil Type	Clay	Clay
Thickness (m)	7.00	18.00
Shear Wave Velocity (m/s)	200	300
Plasticity Index (%)	20	20
Undrained Shear Strength (kPa)	40	100
Modulus of Elasticity (kPa)	150380	339900
Drained Modulus of Elasticity (kPa)	60150	135960
Shear Modulus (kPa)	73000	165000

Within the scope of this study, the surface ground scenarios were labelled with a special coding method. Accordingly, in the triple code system, 'SS' indicates the surface soil and the number next to it indicates the shear wave velocity value (SS1; V_s=100 m/s, SS2; V_s=250 m/s, SS3; V_s=360 m/s). The following values indicate the shear strength and plasticity index values of the soil, respectively. Examples of the code system are presented below:

SS1-20-15: V_s=100 m/s, c_u=20 kPa, PI=%15

SS2-50-20: V_s=250 m/s, c_u=50 kPa, PI=%20

SS3-110-30: V_s=360 m/s, c_u=110 kPa, PI=%30

Table 3. Geotechnical parameters of surface soils

Case	Shear Wave Velocity (m/s)	Plasticity Index (%)	Undrained Shear Strength (kPa)	Modulus of Elasticity (kPa)	Drained Modulus of Elasticity (kPa)	Shear Modulus (kPa)
SS1-20-15	100	15	20	46800	18720	18000
SS1-50-15	100	15	50	46800	18720	18000
SS1-110-15	100	15	110	46800	18720	18000
SS1-20-20	100	20	20	46800	18720	18000
SS1-50-20	100	20	50	46800	18720	18000
SS1-110-20	100	20	110	46800	18720	18000
SS1-20-30	100	30	20	46800	18720	18000
SS1-50-30	100	30	50	46800	18720	18000
SS1-110-30	100	30	110	46800	18720	18000
SS2-20-15	250	15	20	296400	118560	114000
SS2-50-15	250	15	50	296400	118560	114000
SS2-110-15	250	15	110	296400	118560	114000
SS2-20-20	250	20	20	296400	118560	114000
SS2-50-20	250	20	50	296400	118560	114000
SS2-110-20	250	20	110	296400	118560	114000
SS2-20-30	250	30	20	296400	118560	114000
SS2-50-30	250	30	50	296400	118560	114000
SS2-110-30	250	30	110	296400	118560	114000
SS3-20-15	360	15	20	616200	246480	237000
SS3-50-15	360	15	50	616200	246480	237000
SS3-110-15	360	15	110	616200	246480	237000
SS3-20-20	360	20	20	616200	246480	237000
SS3-50-20	360	20	50	616200	246480	237000
SS3-110-20	360	20	110	616200	246480	237000
SS3-20-30	360	30	20	616200	246480	237000
SS3-50-30	360	30	50	616200	246480	237000
SS3-110-30	360	30	110	616200	246480	237000

In addition, the unit volume weight of all soils included in the study was assumed to be 18 kN/m^3 and Poisson's ratio was assumed to be 0.3.

Empirical relationships accepted in the literature were used to calculate some of the soil parameters required for finite element analyses.

Sorensen and Okkels (2013) proposed that the drained shear strength of clay soils can be calculated based on the undrained shear strength, as shown in Eq. (3.1).

$$c' = 0.1 \times c_u \tag{3.1}$$

Here, c' is the drained shear strength and c_u is the undrained shear strength.

Terzaghi et al. (1996) proposed a correlation between the plasticity index of clay soils and the drained shear resistance angle as shown in Figure 23.

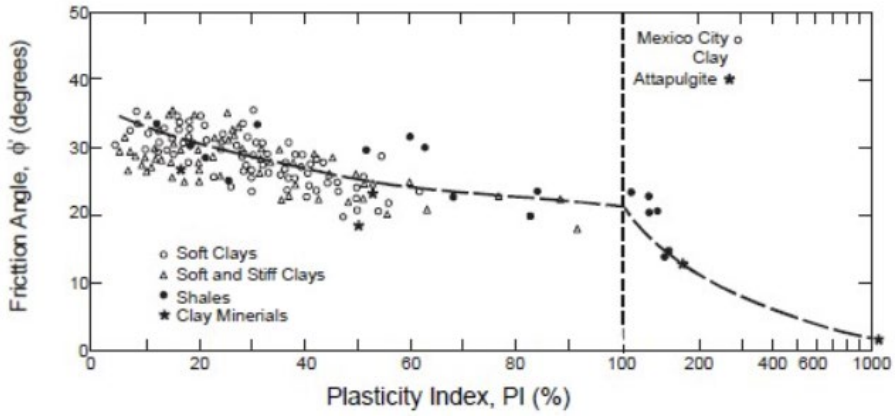

Figure 23. Relation between plasticity index and drained friction angle (Terzaghi et al., 1996)

Butler (1975) proposed the relationship between the deformation modulus with drainage and the deformation modulus without drainage in cohesive soils in accordance with the results obtained from detailed case analyses (see Eq. 3.2).

$$E'_s = \beta \times E_u \quad (3.2)$$

Where E'_s is the modulus of deformation with drainage and E_u is the modulus of deformation without drainage. β' is a correction coefficient depending on the soil type and can be taken from Table 4.

Table 4. Correction coefficient values depending on soil type (Butler, 1975)

Soil Type	**Factor β**
Gravel	0.9
Sand	0.8
Silt, Silty Clay	0.7
Stiff Clay	0.6
Soft Clay	0.4

The shear moduli of the soils have been calculated as a function of the shear wave velocity and the density according to Eq 3.3.

$$G = \delta \times V_s^2 \quad (3.3)$$

Where, G is shear modulus, δ is soil density and V_s is shear wave velocity.

3.2.2. Structural parameters

The concrete parameters summarized in Table 5 were taken into account in the design of the structural features of the underground structure. The walls and top slab have a section thickness of 0.70 m and the bottom slab has a section thickness of 1.00 m. The span of the underground structure is 10.00 m.

Table 5. Material properties of concrete

Modulus of Elasticity (kPa)	32×10^6
Unit Weight (kN/m^3)	25
Poisson's Ratio	0.2

For the infrastructure with a rectangular cross-section, the cross-section with the geometry shown in Figure 24 was considered. In addition, the general view of the structure can be examined in Figure 25.

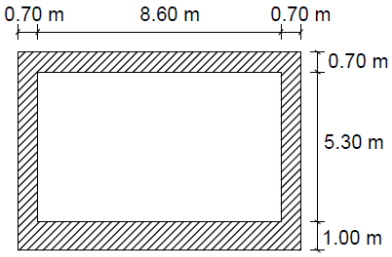

Figure 24. Cross-sectional view of underground structure

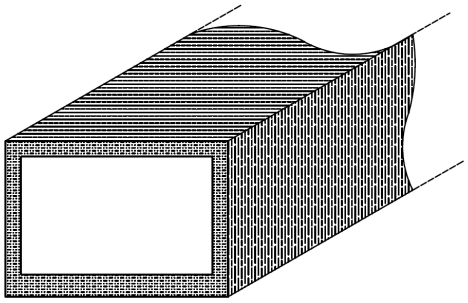

Figure 25. General view of underground structure

The structural parameters have been modelled by means of the 'plate' element model in the finite element method. Plates are beam elements used to model walls, slabs, shells or pavements and allow the modelling of structures in the ground with bending stiffness and normal stiffness (Bentley, 2021).

The finite element software used in this study, Plaxis, has the assumption that the plate elements are continuous in the invisible dimension, which is suitable for structures with large lengths such as tunnels and metro stations.

The behavior of the slabs is represented by the bending stiffness (EI) and the axial stiffness (EA). Equation 3.4 calculates the bending stiffness (EI) of the members.

$$EI = E \times \frac{bh^3}{12} \tag{3.4}$$

The axial stiffness (EA) of the structural members is calculated by Equation 3.5.

$$EA = E \times b \times h \tag{3.5}$$

Where E is the modulus of elasticity of concrete, b and h are the thickness and length of the structure. The material properties are calculated for unit element of 1 m in length under conditions of plane strain.

Table 6. Structural parameters of metro station

Structural Member	**Walls and Top Slab**	**Base Slab**
Plate Thickness (m)	0.70	1.00
Poisson Ratio	0.2	0.2
Flexural Rigidity (kN/m^2/m)	333×10^3	2666×10^3
Normal Stiffness (kN/m)	16×10^6	32×10^6
Weight (kN/m)	7.50	15.00

The relative expression of the racking stiffness of the designed underground structure and the flexibility ratio of the surrounding soil is defined by the flexibility ratio. The flexibility ratio can be calculated as a function of the structural racking stiffness (NHCRP, 2008).

Therefore, the structural racking stiffness of the underground structure was determined using the SAP2000 software. To determine the structural racking stiffness, a unit load was applied at the top slab level of the structure and the response deformations were observed. In the model where the bottom of the structure is constrained against rotation, the joints are left free (see Figure 26). The material properties shown in the Table 6 are used in the structural analysis.

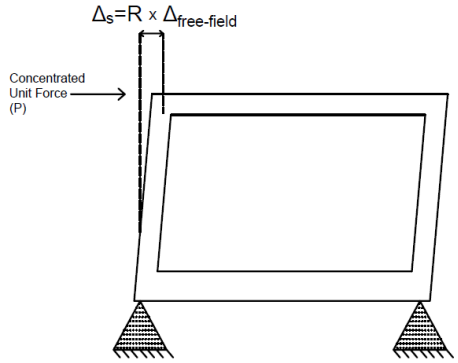

Figure 26. Simplified frame analysis of structural racking stiffness (NHCRP, 2008)

The calculated unit load represents the deformation capacity of the structure. To calculate the flexibility ratio of the structure, the deformation capacity of the soil is compared with the deformation capacity of the structure using Equation 3.6.

$$F = \frac{G_{rep} \times W}{H \times f} \tag{3.6}$$

Where H is the structural height, f is the unit load causing unit deformation and W is the structural width. G_{rep} is the representative shear modulus of the soil profile and is calculated from equation 3.7.

$$\frac{1}{G_{rep}} = \frac{\sum_{i=1}^{n} \frac{H_i}{G_i}}{\sum_{i=1}^{n} H_i} \tag{3.7}$$

Here, H and G are the height and shear modulus of each different soil layer, respectively.

The calculated representative shear modulus values and corresponding flexibility ratios for each different surface soil scenario can be analysed in Table 7.

Table 7. Flexibility ratios for different surface soil cases

Case	**$G_{surface\ soil}$ (kPa)**	**G_{rep} (kPa)**	**Flexibility Ratio (F)**
SS1-20-15			
SS1-50-15			
SS1-110-15			
SS1-20-20			
SS1-50-20	18000	61618	1.194
SS1-110-20			
SS1-20-30			
SS1-50-30			
SS1-110-30			
SS2-20-15			
SS2-50-15			
SS2-110-15			
SS2-20-20			
SS2-50-20	114000	118600	2.297
SS2-110-20			
SS2-20-30			
SS2-50-30			
SS2-110-30			
SS3-20-15			
SS3-50-15			
SS3-110-15			
SS3-20-20			
SS3-50-20	237000	130328	2.525
SS3-110-20			
SS3-20-30			
SS3-50-30			
SS3-110-30			

3.2.3. Input Motion

The Tabas earthquake, with a peak ground acceleration of 0.862, was used as the seismic input in the study. This was done to clearly describe the change in the effect of the surface soil effect on the seismic response of the infrastructure with the order of earthquake motion. The earthquake record used in the analyses was selected from the Pacific Earthquake Engineering Research Center (PEER) shaking database (https://ngawest2.berkeley.edu, last accessed June, 2024). The motion parameters are listed in Table 8. The acceleration, velocity and deformation plots are shown in Figure 27.

Table 8. Properties of selected input motions

Event Name	PGA (g)	Magnitude	Rupture Distance (km)	V_{s30} (m/s)
Tabas Earthquake	0.862	7.3	2.05	767

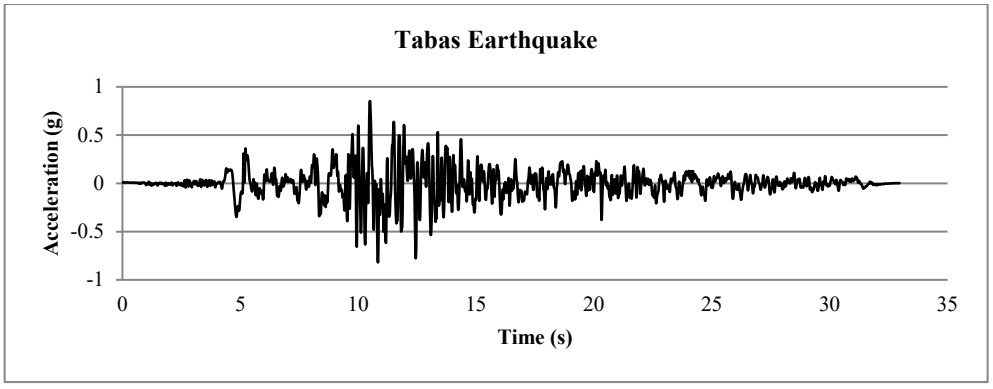

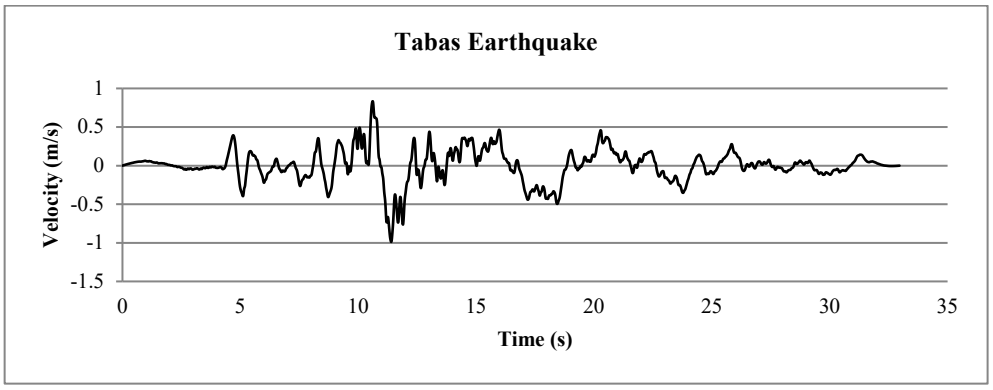

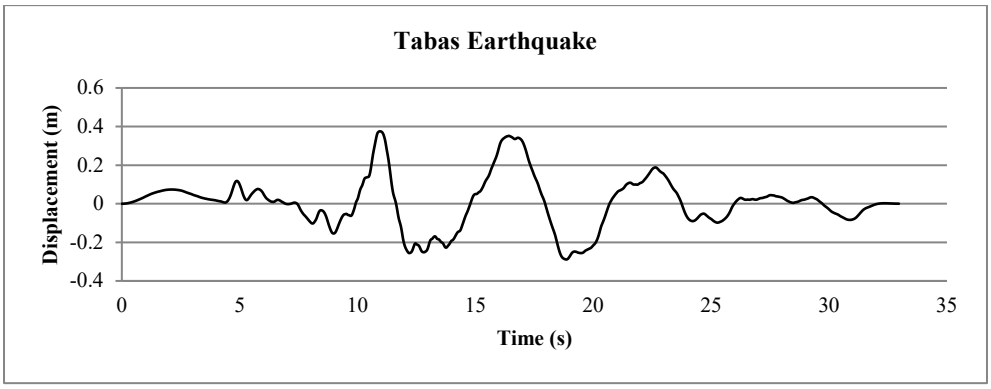

Figure 27. Acceleration, velocity and displacement time histories of Tabas Earthquake

3.3. Free-Field Site Response Analyses

Vertically propagating shear waves induced by earthquakes are recognized as the main cause of racking deformations in underground structures (Wang, 1993). Codes based on one-dimensional wave transmission theory are applied to predict the free field shear deflections and shear modulus reductions of the ground, resulting in racking deformations in the structure. In this study, DEEPSOIL software was used to perform one-dimensional equivalent linear free field soil response analyses.

One-dimensional soil response analyses can be performed using three different methods (Hashash, 2024):

i. Linear time and frequency domain analyses,

ii. Equivalent linear frequency domain analyses,

iii. Non-linear time domain analyses.

In this study, the Equivalent Linear Analysis (EL) method was used, which uses an iterative procedure to recreate the shear modulus and damping ratio of the soil at each cyclic loading. Equivalent Linear Analysis defines the G/G_{max} and damping ratio of the soil as a function of shear deformation (Hashash, 2024). A simplified representation of the one-dimensional equivalent linear soil response analysis is shown in Figure 28.

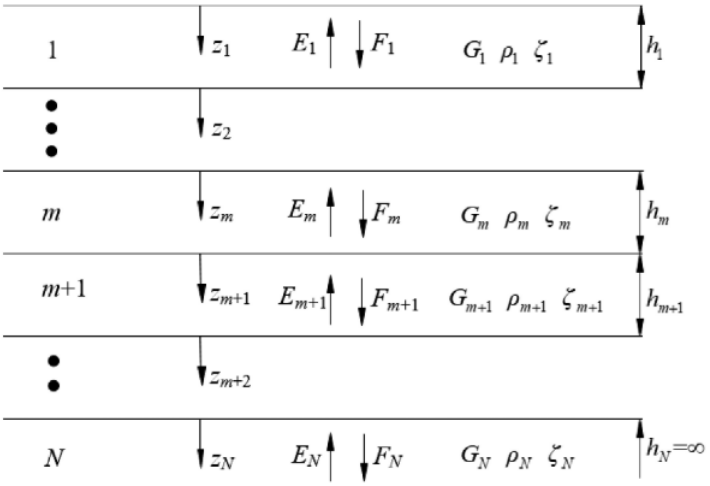

Figure 28. Simplified procedure of one dimensional equivalent linear ground response analysis (Schnabel, Lysmer and Seed, 1972)

As shown in Figure 28, the response of each soil layer is predicted by a number of critical parameters; soil layer thickness (h), density (δ), shear modulus (G) and damping ratio (ζ) of the soil (Schnabel, Lysmer and Seed, 1972). The soil parameters used in this study were presented in the previous section (see Table 2 and Table 3).

With increasing shear deformation, most soils rapidly lose their shear stiffness. This means that they exhibit non-linear behavior when subjected to large shear stresses. Under repeated loading, such as that caused by earthquakes, the soil will exhibit hysteretic behavior due to the loading and unloading effect. This means that the rate of damping of the material becomes independent of the frequency. Some researchers have developed some approaches to describe the loading-unloading response of the soil (Masing, 1926).

The stress-strain relationship of the soil during the unloading cycle is not similar to that during the loading cycle. This is due to the non-linear nature of the soil. The hysteretic behavior of the soil is governed by the loading-unloading behavior and causes the shear modulus to decrease with increasing deformation. Therefore, the strain-shear modulus relation and the definition of attenuation are key parameters to simulate the non-linear behavior of the soil (Masing, 1926).

The reference curves proposed by Vucetic and Dobry (1991) have been used to model the decreasing G/G_{max} and increasing damping ratio in parallel with the increasing shear deformation of clay units. The main factor in the choice of this reference curve is that it provides a suitable prediction with less complex input than other reference curves.

In principle, the plasticity index of the clay unit is required for this reference curve proposed by Vucetic and Dobry (1991). This means that the relationship between G/G_{max} and shear deformation is assumed to be substantially modified by the plasticity index of the cohesive soil (see Figure 29).

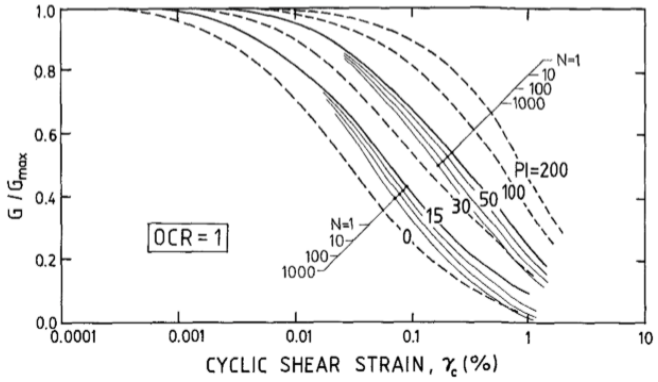

Figure 29. G/G_{max} versus cyclic shear strain (γ_c) curve for soils with different plasticity indices (Vucetic and Dobry, 1991)

An example of the attenuation curve of one-dimensional soil modelled in DEEPSOIL software is presented in Figure 30.

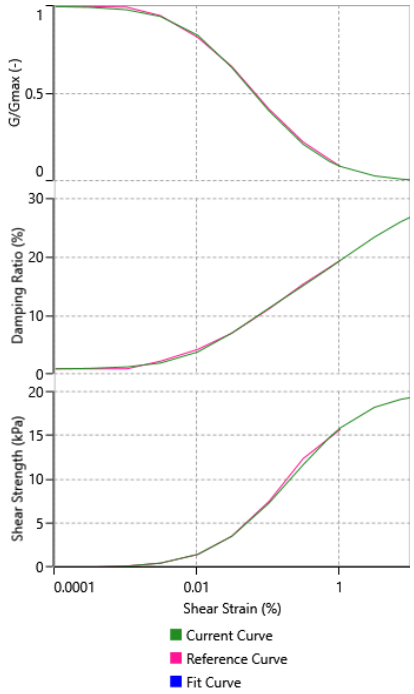

Figure 30. Degradation curves of Surface Soil 1

The shear wave velocities and thicknesses of the identified soil layers were used to subdivide each layer into sublayers. The target frequency (f_{max}) was then determined. The study used 30 Hz as the target frequency, following values of 30 Hz or higher which are often recommended in the literature (Hashash, 2024). Analyses therefore continued with equal maximum frequency subgrades along the soil profile (see Figure 31).

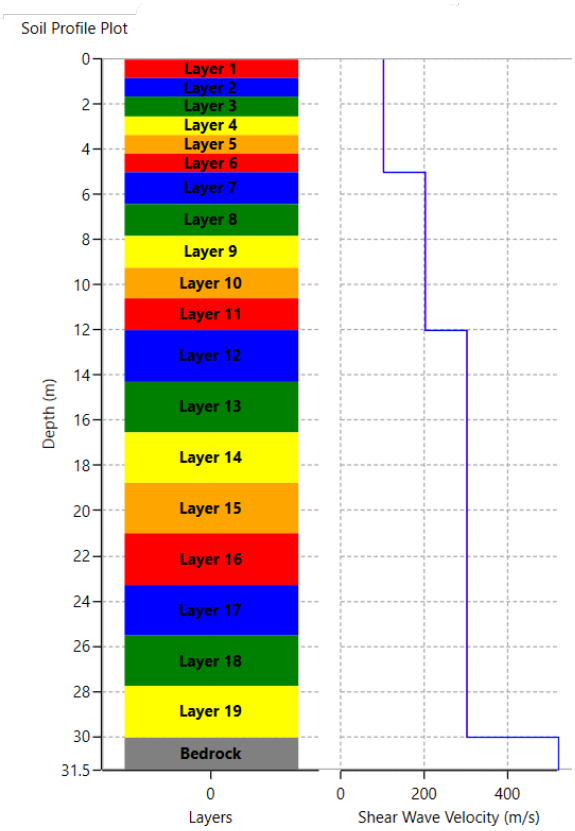

Figure 31 Overview of sublayers used in DEEPSOIL for Surface Soil 1 case

The bedrock was defined below the 30 m ground profile used in the one-dimensional ground response analyses. As the seismic inputs used were outcrop motion and the properties shown in Figure 32 were used, the bedrock was defined as an elastic half-space. A damping ratio of 2%, commonly used in the literature, was considered as the effect of bedrock damping ratio is negligible in frequency domain analyses (Hashash, 2024).

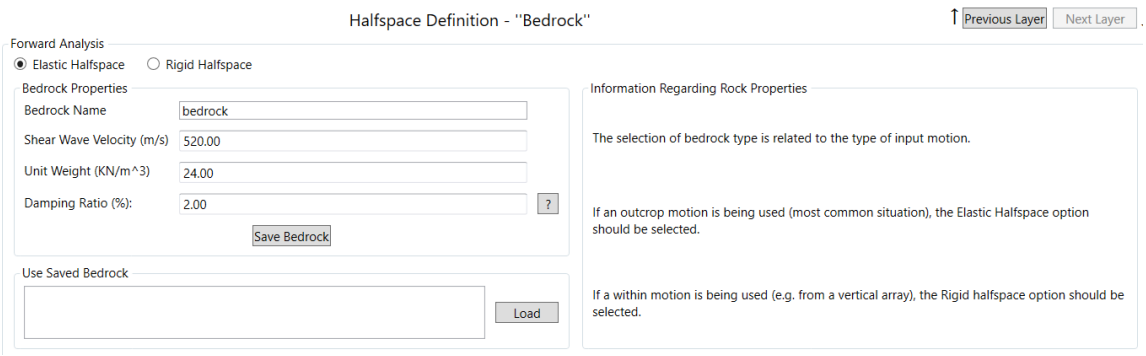

Figure 32. Bedrock parameters used in DEEPSOIL

3.4. Soil-Structure Interaction Analyses

PLAXIS is a finite element software developed for deformation and stability analysis in geotechnical engineering and is widely used in geotechnical applications today. The software uses soil models to simulate soil behavior. The most critical elements for realistic modelling of the geotechnical problem are the model boundaries, the soil models and the definition of the appropriate meshes (Bentley Systems, 2021).

If the model boundaries used in the program are larger than required, the soil deformations between the structure and the model boundary may be damped. Alternatively, if the model boundaries are smaller than required, the deformations may be magnified differently than in reality (Wang, 1993; Huo et al., 2005).

A number of preliminary runs were carried out using different model boundaries to eliminate the effects of model boundaries. In the analyses of structure-soil interaction, the model boundaries where horizontal deformation is equal to free field deformation of soil were used in further analyses (see Figure 33).

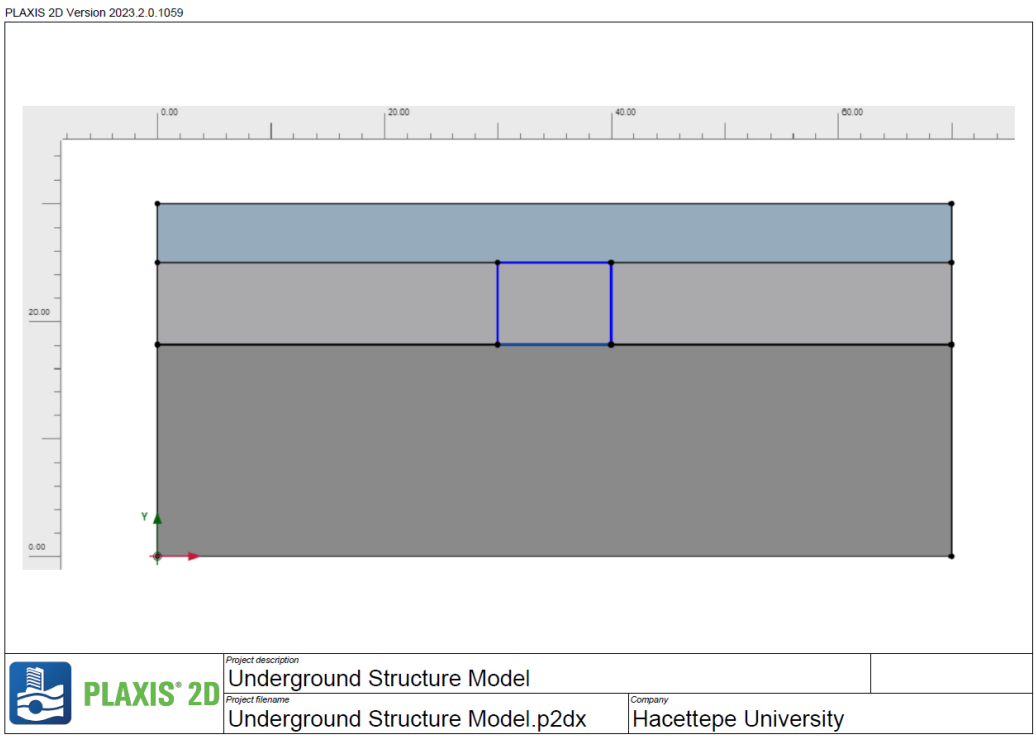

Figure 33. Dimensions of finite element model

The Hardening Soil model represents the behavior of the soil under applied deformations in the finite element model. This soil model has been developed to describe the behavior of both soft soils and stiff soils. When the soil is subject to primary deviatoric loading, there is a loss of stiffness in parallel with the development of permanent deformation. In order to realistically represent this deviatoric loading behavior, the hardening soil model uses several soil parameters (Schanz et al., 1999).

The analyses used the soil parameters presented in the relevant section. A Poisson's ratio of 0.3 was also assumed for clay, and the values of the stress-dependent coefficient (m) and the angle of dilatancy left at their default values.

In the two-dimensional analyses, the deformations applied to the model boundaries were calibrated to ensure that the free field deformation obtained at the centre of the model was close to the free field conditions. These calibrated deformations were applied to the model boundaries. For each surface soil scenario, the free field deformations were specifically evaluated and applied to the model as linear deformations at intervals corresponding to the deformation changes obtained from one-dimensional soil response analyses. The baseline of model was fixed in analyses.

The mesh, which is another important parameter in structure-soil interaction models, was then generated using the experience gained from the preliminary analyses, as shown in Figure 34.

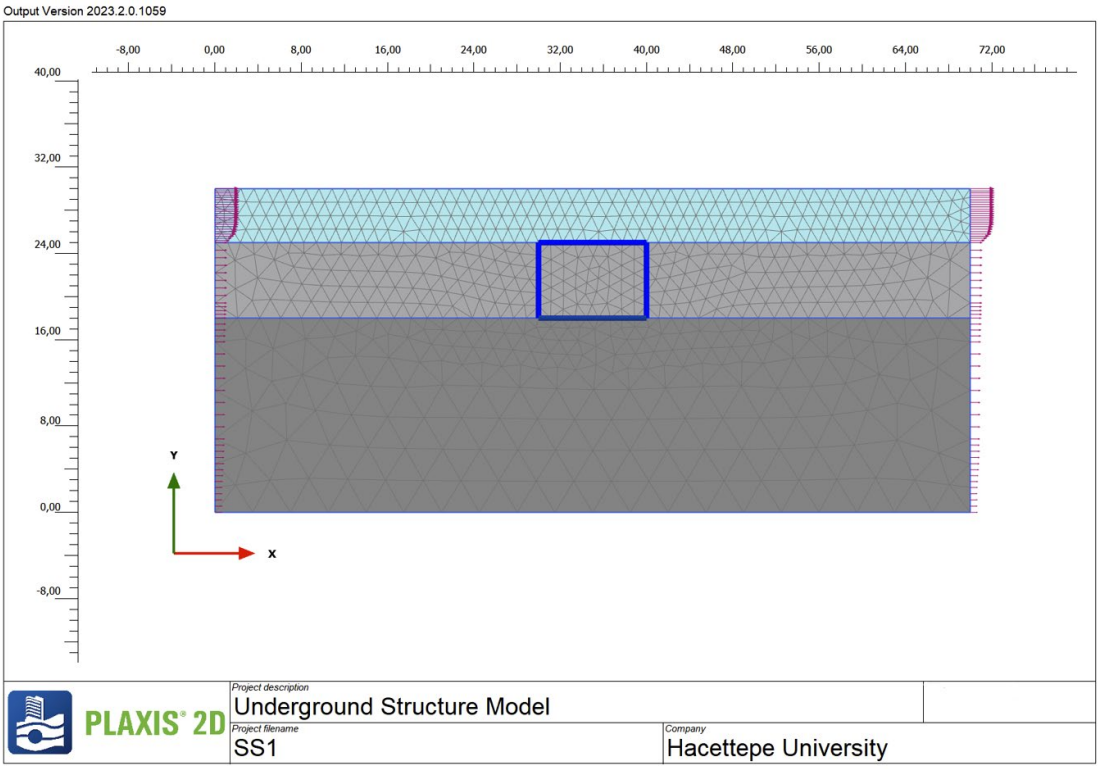

Figure 34. Mesh used in finite element analyses

The analyses were essentially carried out using two different procedures. In the first part, the K_0 procedure, which represents the natural state of the soil, was carried out and free field deformations were applied to the soil in its natural state. This verified that the deformations acting on the structure were close to the deformations that the soil would undergo under free field situation. In other part, the structural components was activated and the free field deformations were applied to the structure-soil model (see Figure 35 for stages).

(a)

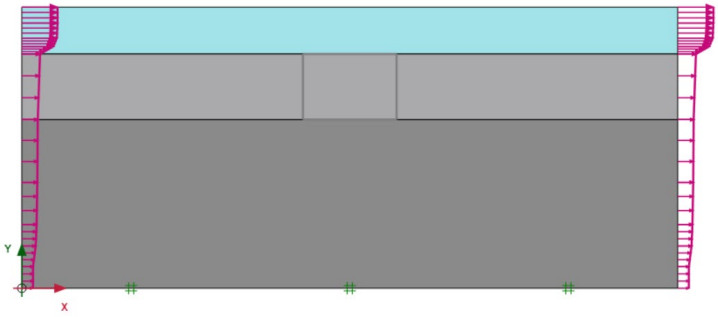

(b)

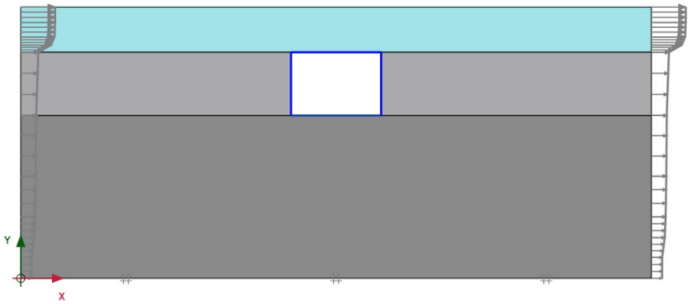

(c)

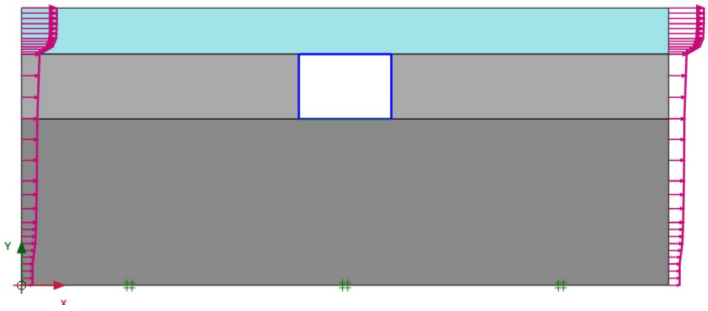

Figure 35. Steps of soil structure interaction analyses a) K_0 procedure, b) free-field response analysis, b) installation of structure, c) implementation of deformations

4. RESULTS

27 different surface soil scenarios, the horizontal displacements obtained as a result of one-dimensional ground response analyses are shown in Figure 36.

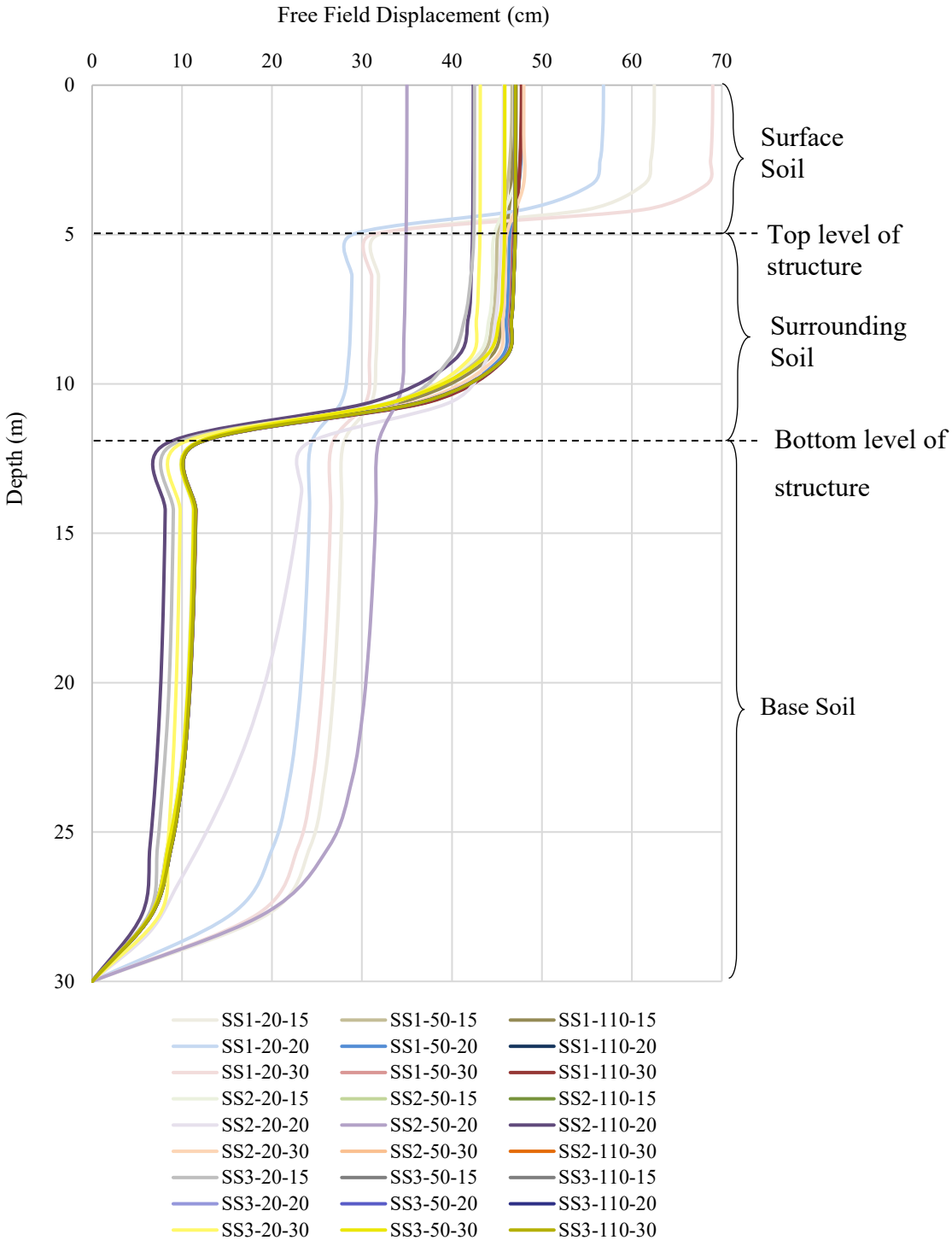

Figure 36. Free-field displacements of different surface soil cases

As can be seen in Figure 36, the deformations change visibly at the layer boundaries where the stiffness changes. In addition, the deformations at the soil surface increase significantly as the surface soil stiffness decreases. The soil amplification values increase as the soil stiffness decreases.

The following plots are presented for the variation of structural and free field racking deformations with variation of the shear strength, shear wave velocity and plasticity index of the surface soil (see Figure 37~Figure 42). Deformations shown here reflect relative deformation results at levels corresponding to upper and lower levels of structure for free field condition and structure-soil interaction condition.

The results obtained by comparing the relative deformation values with the varying surface soil parameters for free field and structure-ground interaction conditions can be listed as follows:

- The most critical parameter affecting the relative deformation along the height of the structure in both free field and structure-ground interaction conditions is shear strength of surface soil.

- The shear wave velocity and plasticity index of surface soil have a relatively limited effect on the deformation behavior.

- The increase in deformation in surface soil scenarios with varying shear wave velocity and plasticity index is parallel to change in shear strength in these scenarios.

These results are only obtained from the analyses performed with a relatively surface buried single span underground structure model in cohesive soil. Normalized racking deformations are presented in next section to clearly demonstrate effect of surface soil parameteres on seismic deformation of structure.

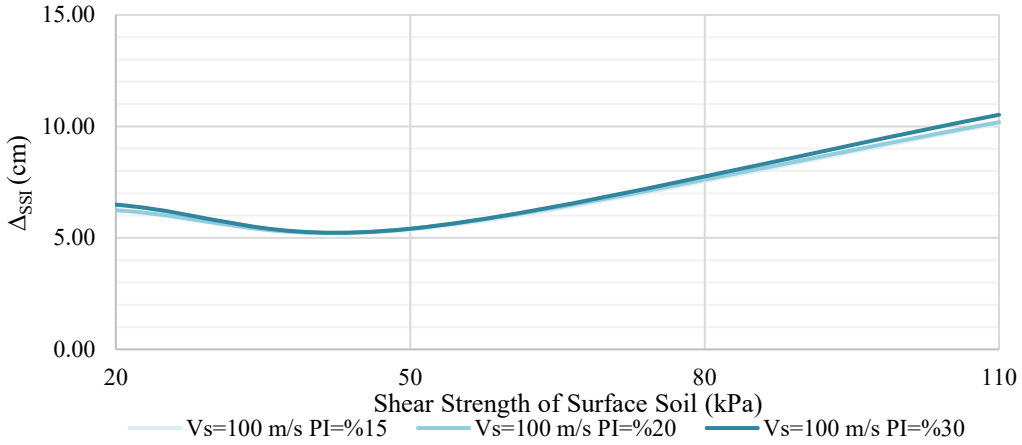

(a)

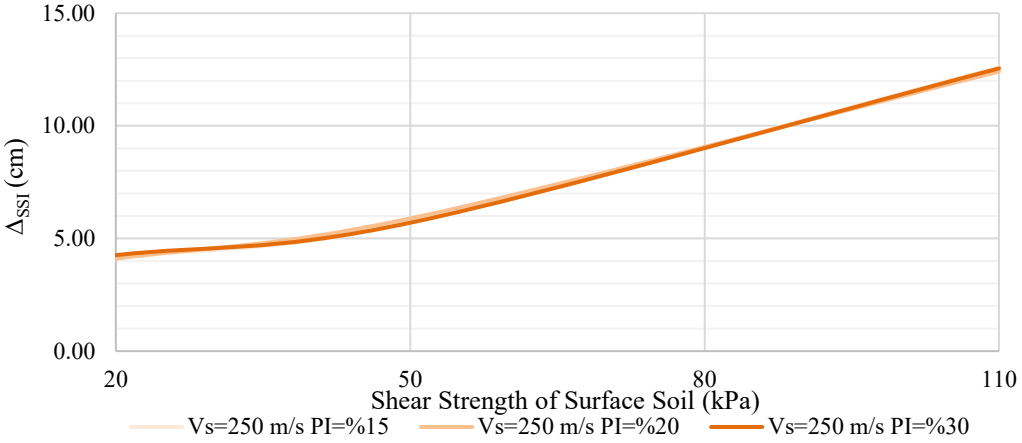

(b)

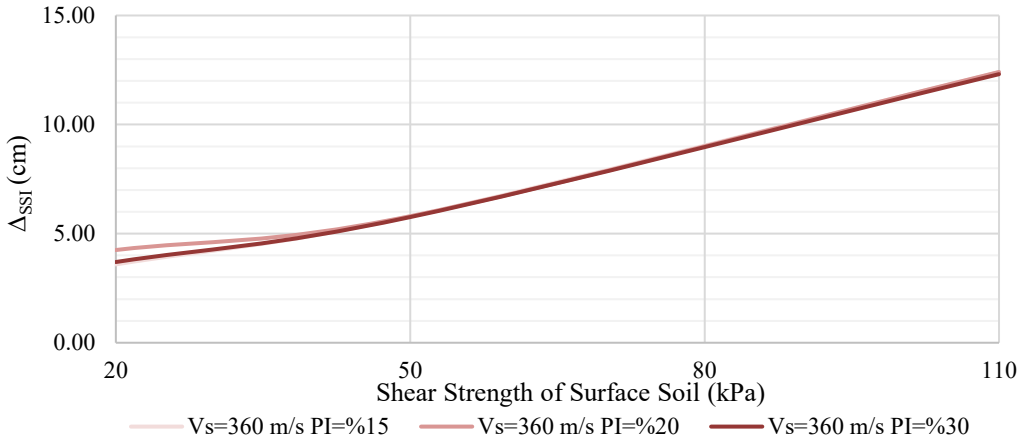

(c)

Figure 37. Variation of structural racking deformations with the variation of surface soil shear strength (a) shear strength of surface soil is 20 kPa, (b) shear strength of surface soil is 50 kPa, (c) shear strength of surface soil is 110 kPa

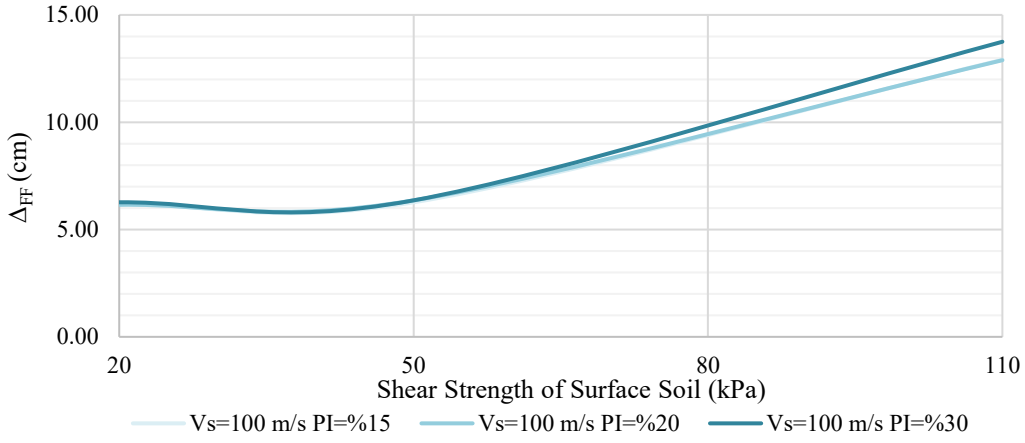

(a)

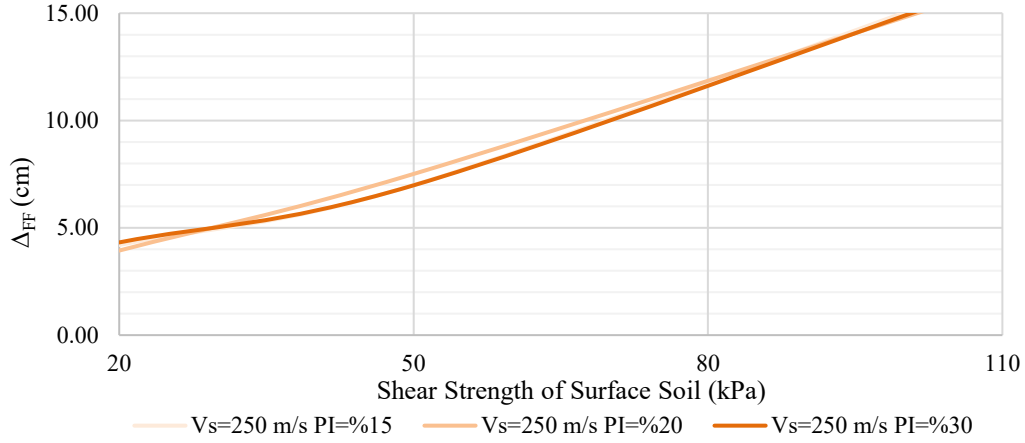

(b)

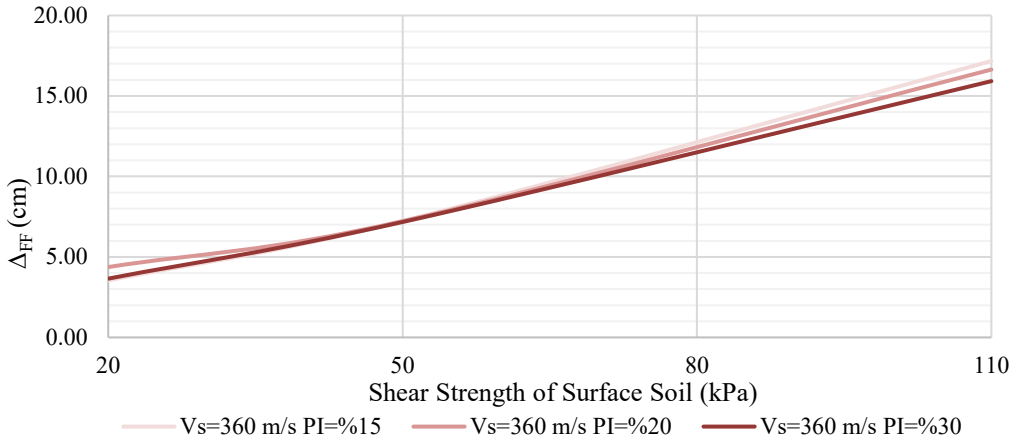

(c)

Figure 38. Variation of free field racking deformations with the variation of surface soil shear strength (a) shear strength of surface soil is 20 kPa, (b) shear strength of surface soil is 50 kPa, (c) shear strength of surface soil is 110 kPa

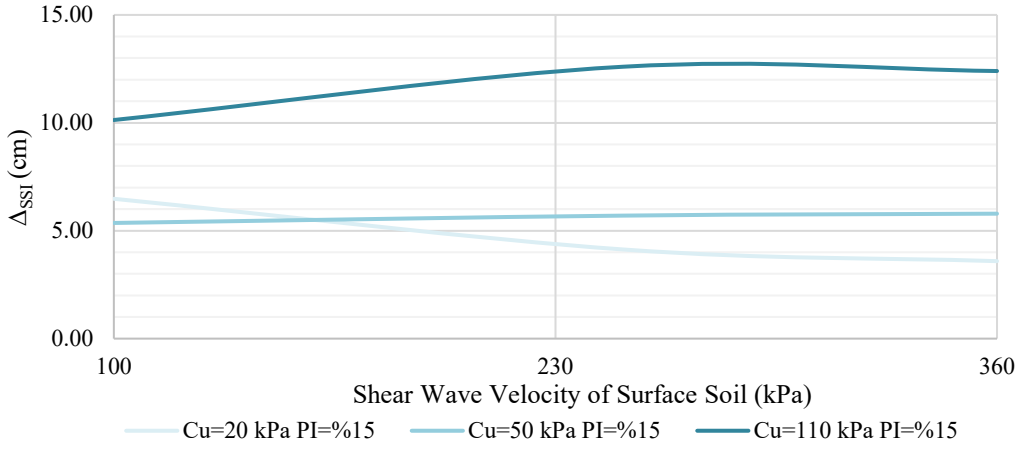

(a)

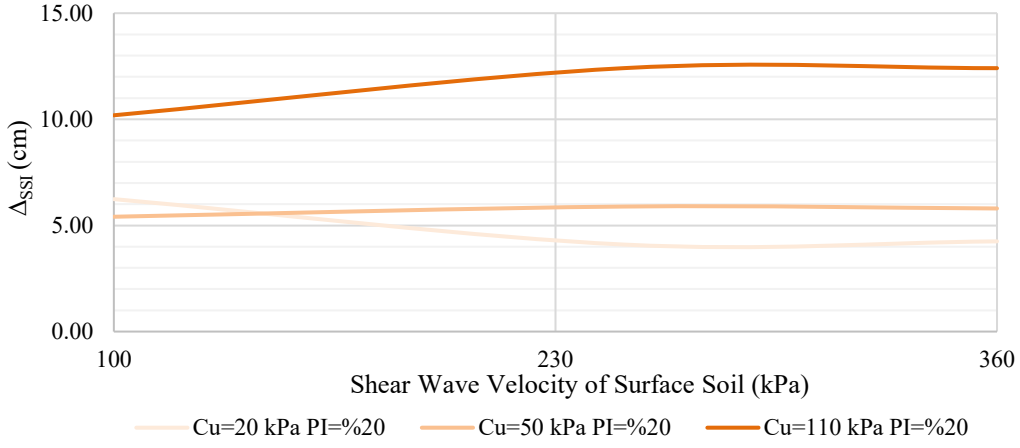

(b)

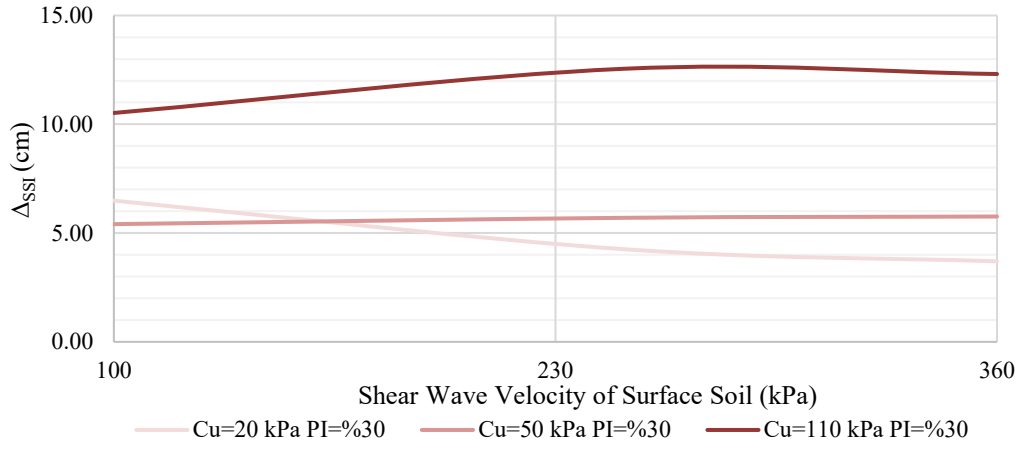

(c)

Figure 39. Variation of structural racking deformations with the variation of surface soil shear wave velocity (a) shear wave velocity of surface soil is 100 m/s, (b) shear wave velocity of surface soil is 250 m/s, (c) shear wave velocity of surface soil is 360 m/s

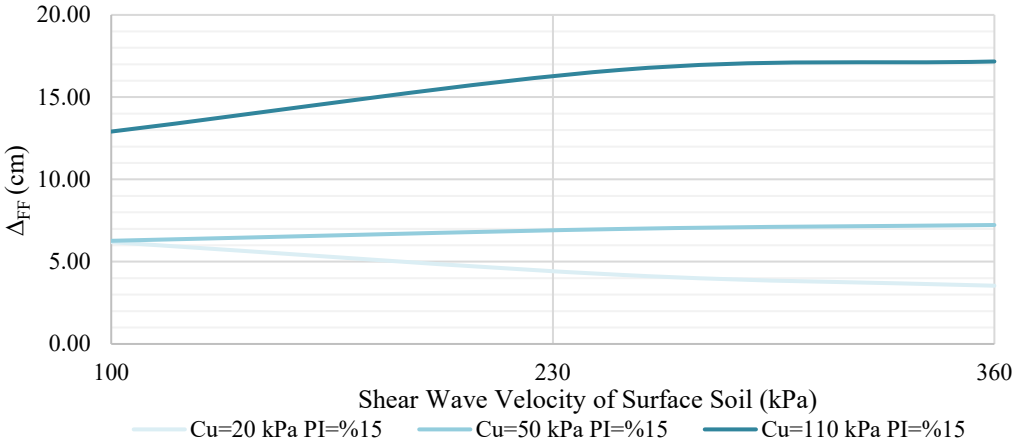

(a)

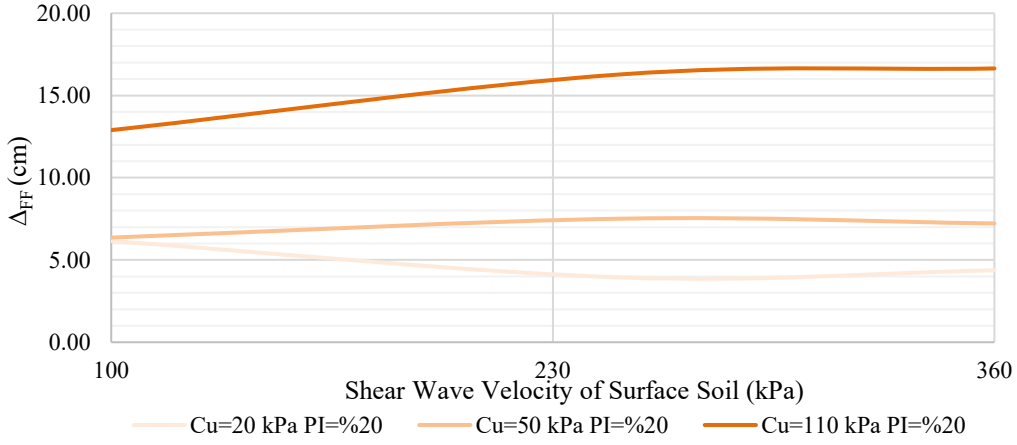

(b)

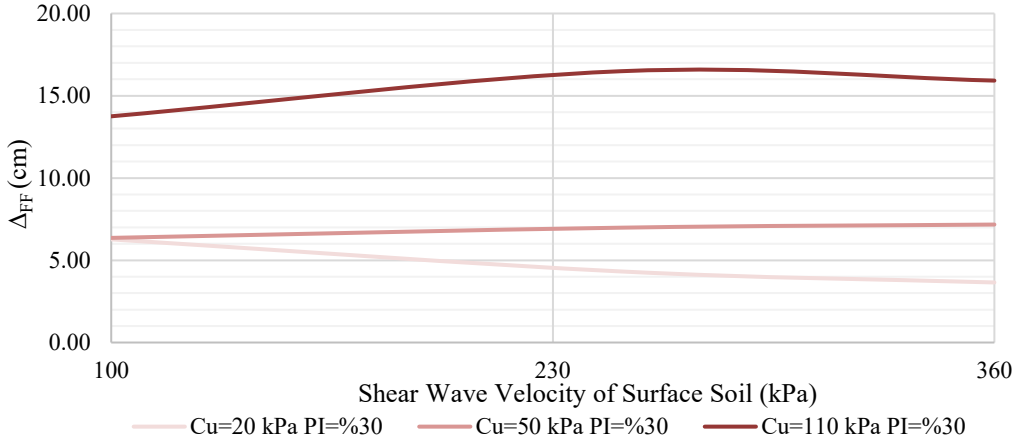

(c)

Figure 40. Variation of free field racking deformations with the variation of surface soil shear wave velocity (a) shear wave velocity of surface soil is 100 m/s, (b) shear wave velocity of surface soil is 250 m/s, (c) shear wave velocity of surface soil is 360 m/s

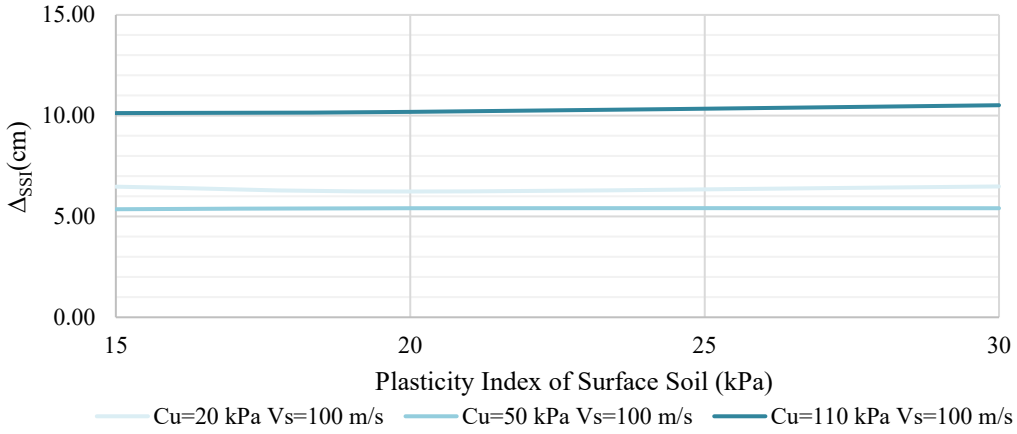

(a)

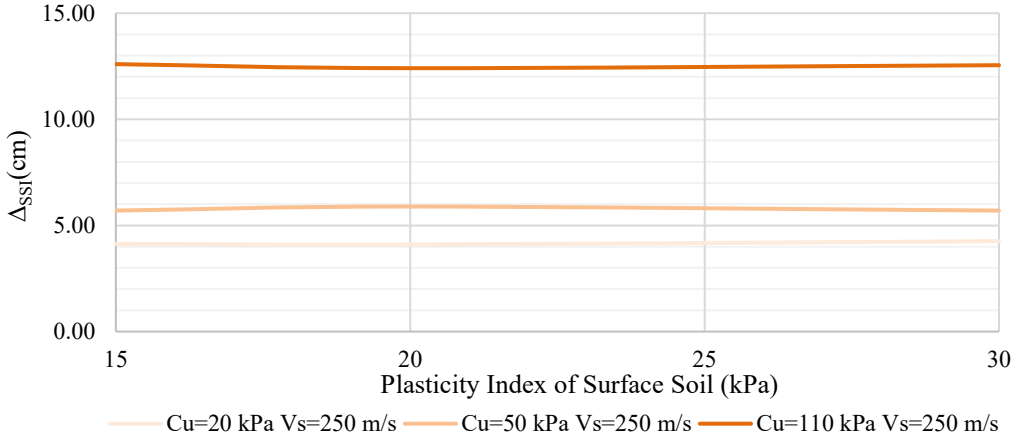

(b)

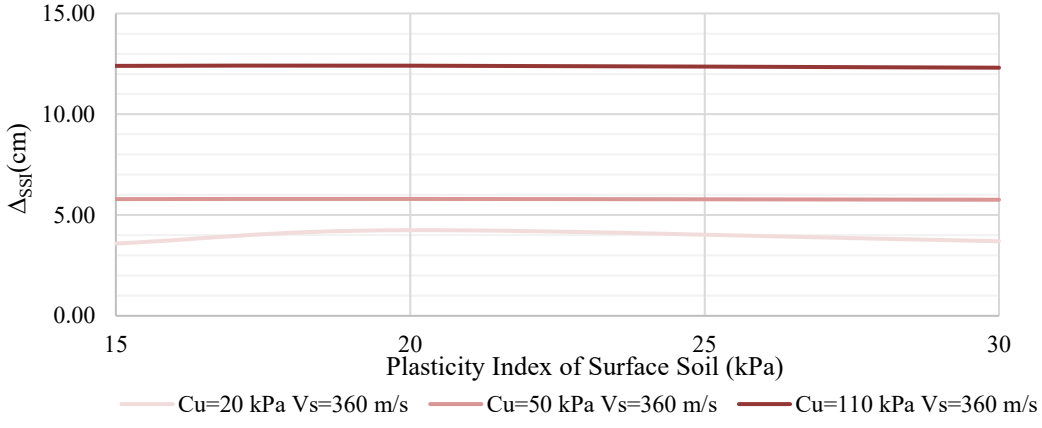

(c)

Figure 41. Variation of structural racking deformations with the variation of surface soil plasticity index (a) plasticity index of surface soil is %15, (b) plasticity index of surface soil is %20, (c) plasticity index of surface soil is %30

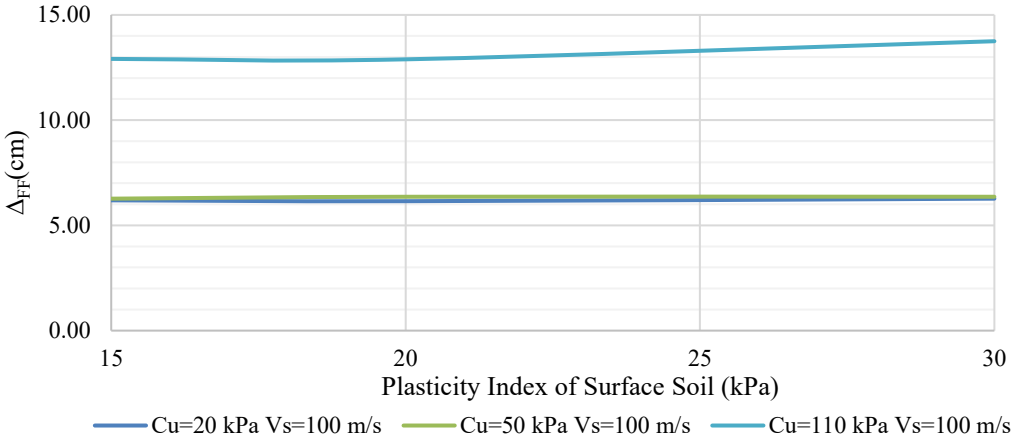

(a)

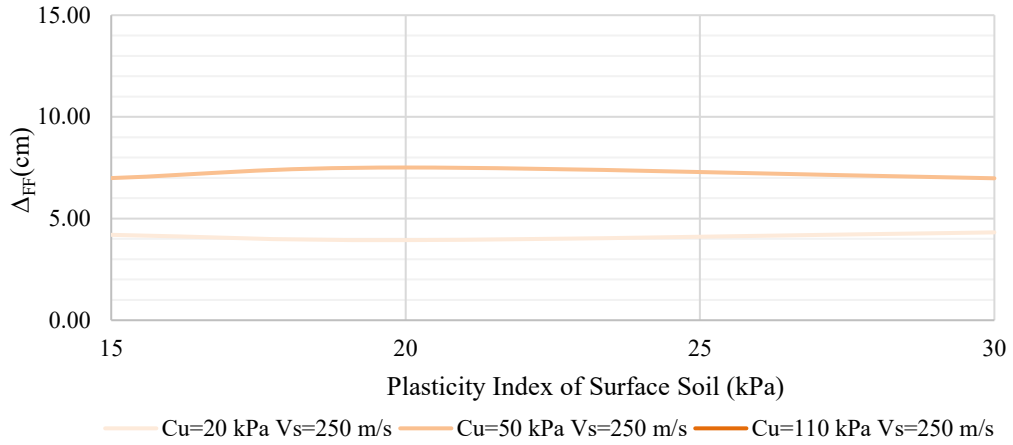

(b)

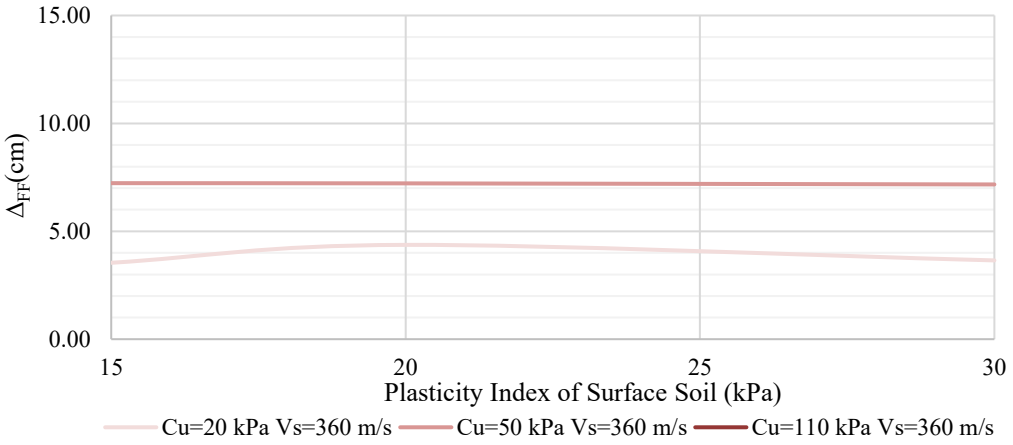

(c)

Figure 42. Variation of free field racking deformations with the variation of surface soil plasticity index (a) plasticity index of surface soil is %15, (b) plasticity index of surface soil is %20, (c) plasticity index of surface soil is %30

The structural racking deformations presented in the previous graphs were normalized to the free field deformations and the variation in surface soil properties and racking ratio were determined as shown in figures.

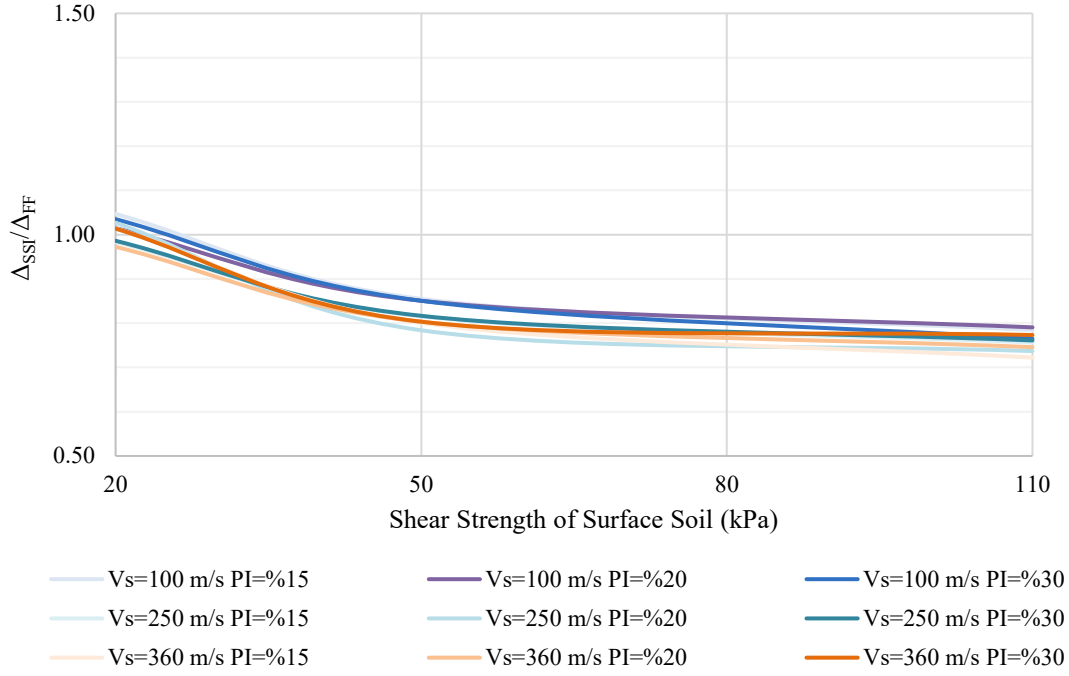

Figure 43. Variation of racking ratio with shear strength of surface soil

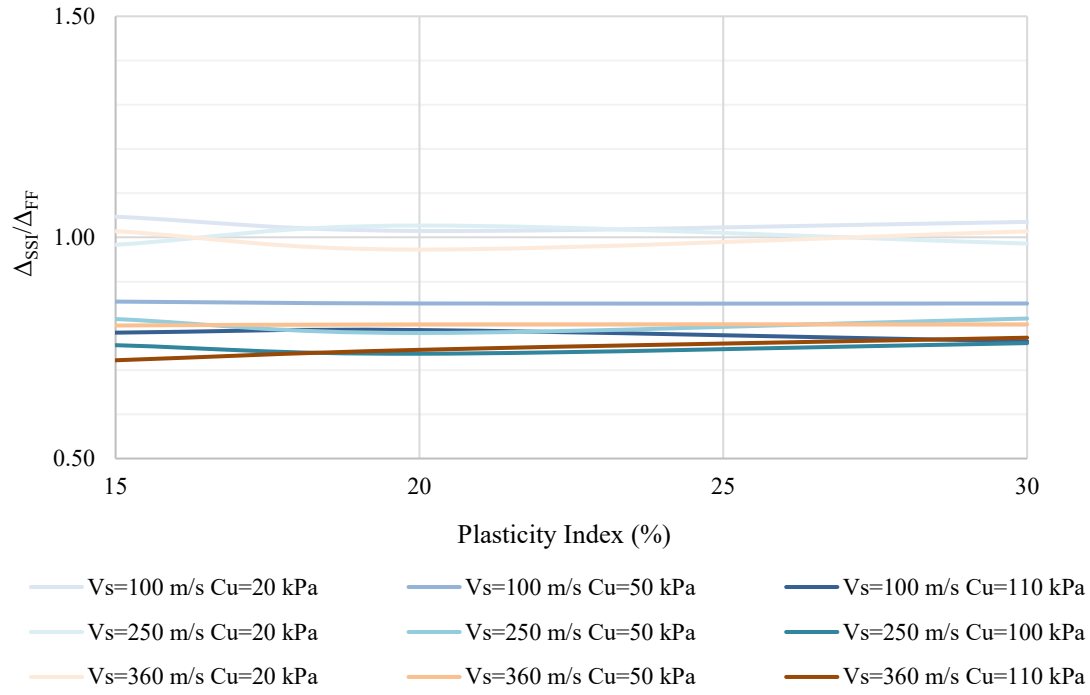

Figure 44. Variation of racking ratio plasticity index of surface soil

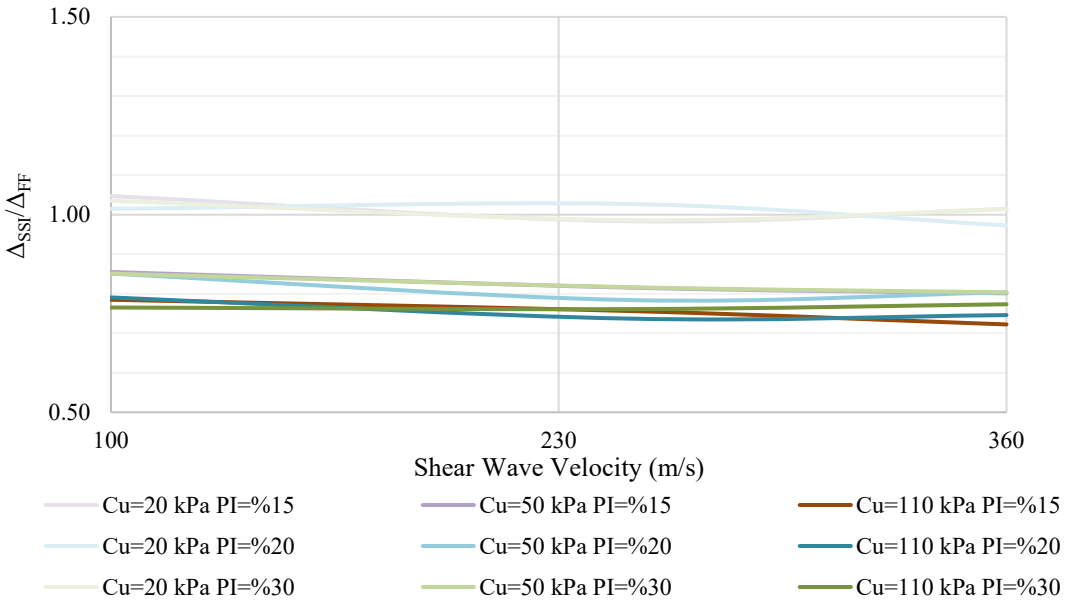

Figure 45. Variation of racking ratio with shear wave velocity of surface soil

5. CONCLUSIONS

A comprehensive numerical study of the deformations experienced by a single-span rectangular substructure buried in cohesive soil during a strong earthquake is presented. The pseudo-static method is used to investigate the deformation behavior of the structure, with one-dimensional analyses performed using DEEPSOIL software and two-dimensional analyses performed using PLAXIS software. As a result of the analyses using 27 different surface soil scenarios, effect of change in shear strength, shear wave velocity and plasticity index of surface soil on the deformations experienced by the structure was investigated.

The outcomes can be encapsulated as follows:

1. The seismic deformation characteristics of infrastructures vary significantly with the characteristic parameters of the surface soil.
2. As the shear strength of the surface soil increases, the racking ratio decreases, even if the magnitude of the deformation experienced increases.
3. For soils with the same shear strength and plasticity index but different shear wave velocities, the shear wave velocity has no significant effect on the racking ratio.
4. For soils with the same shear strength and shear wave velocity but different plasticity index, the plasticity index has no significant effect on the racking ratio.
5. However, for different shear wave velocity and plasticity index characteristics, the racking ratio decreases with increasing shear strength of the surface soil.
6. In cases with relatively stiff surface soils, the amount of racking, which is the most critical type of deformation of a rectangular substructure, decreases.

On the basis of these results, the following needs for further investigation are identified:

- The seismic behavior of infrastructures with varying surface soil parameters can be investigated by dynamic analyses, where the soil behavior under repeated loading cycles of earthquakes can be well investigated but requires intensive computational effort.

- Laboratory and/or field experiments on scaled models can be used to describe the load transfer mechanism between the surface soil and the structure in detail.
- Effects such as groundwater effects and arching, which are not considered in this study, can be evaluated.

6. REFERENCES

Anderson, D. G., Martin, G. R., Lam, I., & Wang, J. N. (2008). NCHRP Report 611: Seismic analysis and design of retaining walls, buried structures, slopes, and embankments. Transportation Research Board.

Andreotti, G., & Lai C G. (2015). The role of overburden stress on the seismic vulnerability of deep tunnels. Proceedings of the XVI ECSMGE Geotechnical Engineering for Infrastructure and Development, 393–399.

Bentley Systems. (2021). PLAXIS CONNECT Edition V22.00 General Information Manual. www.bentley.com

Bentley. (2021). PLAXIS 2D-Reference Manual.

Cilingir, U., & Madabhushi, S. P. G. (2011). Effect of Depth on the Seismic Response of Square Tunnel. Soils and Foundations, 51(3), 449-457.

Golshani, A., & Rezaeibadashiani, M. (2020). A Numerical Study on Parameters Affecting Seismic Behavior of Cut and Cover Tunnel. Geotechnical and Geological Engineering, 38(2), 2039–2060. https://doi.org/10.1007/s10706-019-01147-x

Hashash, Y. M. A. (2024). DEEPSOIL (2024, V7.0), A Nonlinear and Equivalent Linear Seismic Site Response of One-Dimensional Soil Columns, User Manual. http://deepsoil.cee.illinois.edu/

Hashash, Y. M. A., Hook, J. J., Schmidt, B., & Yao, J. I.-C. (2001). Seismic design and analysis of underground structures. Tunnelling and Underground Space Technology, 16(4), 247-293. https://doi.org/https://doi.org/10.1016/S0886-7798(01)00051-7

Hashash, Y. M. A., Karina, K., Koutsoftas, D., & Riordan, N. O. (2010). Seismic Design Considerations for Underground Box Structures.

https://ngawest2.berkeley.edu, last accessed on June, 2024.

Huo, H., Bobet, A, Fernández, G, & Ramírez, J. (2005). Load Transfer Mechanisms between Underground Structure and Surrounding Ground: Evaluation of the Failure of the Daikai Station. Journal of Geotechnical and Geoenvironmental Engineering, 131(12), 1522-1533. https://doi.org/10.1061/ASCE1090-02412005131:121522

Hwang, R. N., & Lysmer, J. (1981). Response of Buried Structures to Travelling Waves. Journal of the Geotechnical Engineering Division, 107(2). https://doi.org/https://doi.org/10.1061/AJGEB6.0001096

Iıda, H., Hiroto, T., Yoshıda, N., & Iwafuji, M. (1996). Damage to Daikai Subway Station. Soils and Foundations, Special Issue, 283-300.

Li, W., & Chen, Q. (2020). Effect of vertical ground motions and overburden depth on the seismic responses of large underground structures. Engineering Structures, 205. https://doi.org/10.1016/j.engstruct.2019.110073

Lu, C. C., & Hwang, J. H. (2017). Implementation of the modified cross-section racking deformation method using explicit FDM program: A critical assessment. Tunnelling and Underground Space Technology, 68, 58–73. https://doi.org/10.1016/j.tust.2017.05.014

Masing, G. (1926). Eigenspannungen und Verfestigung beim Messing. Proceedings, of Second International Congress of Applied Mechanics, 332-335.

Monsees, J.E., & Merritt, J.L. (1988). Seismic modelling and design of underground structures. Numerical Methods in Geomechanics, 1833-1842

Newmark, N. M. (1967). Problems in Wave Propagation in Soil and Rock. Symposium on Wave Propagation and Dynamic Properties of Earth Materials.

Owen, G. N., & Scholl, R. E. (1981). Earthquake engineering of large underground structures (FHWA/RD-80/195).

Penzien, J. (2000). Seismically induced racking of tunnel linings. Earthquake Engineering and Structural Dynamics, 683-691.

Pitilakis, K., & Tsinidis, G. (2010). Seismic Design of Large, Long Underground Structures: Metro and Parking Stations, Highway Tunnels. International Geotechnical Conference "Geotechnical Challenges of Megacities" GeoMos. https://www.researchgate.net/publication/269809699

Poulos, H. G., & Small, J. C. Development of design charts for concrete pavements and industrial ground slabs (pp. 39–70).

Schanz, T., Vermeer, P. A., & Bonnier P G. (1999). The Hardenind Soil Model: Formulation and Verification. Beyond 2000 in Computational Geotechnics – 10 Years of PLAXIS.

Schnabel, P. B., Lysmer, J., & Bolton Seed, H. (1972). A Computer Program for Earthquake Response Analysis of Horizontally Layered Sites.

Sharma, S., & Judd, W. R. (1991). Underground opening damage from earthquakes. Engineering Geology, 30, 263-276.

Shawkyi, A., & Koichi, M. (1996). Nonlinear Response of Underground RC Structures Under Shear. J. Materials, Conc. Struct., Pavements, 31(538), 195–206.

Sorensen, K. K., Sorensen, K. K., & Okkels, N. (2013). Correlation between drained shear strength and plasticity index of undisturbed overconsolidated clays. 18th International Conference on Soil Mechanics and Geotechnical Engineering. https://www.researchgate.net/publication/285583666

St John, C. M., & Zahrah, T. F. (1987). Aseismic Design of Underground Structures. Tunnelling and Underground Space Technology, 2(2), 165-197.

Terzaghi, K., Peck, R. B., & Mesri, G. (1996). Soil Mechanics in Engineering Practice. John Wiley & Sons, Inc.

Tsinidis, G., de Silva, F., Anastasopoulos, I., Bilotta, E., Bobet, A., Hashash, Y. M. A., He, C., Kampas, G., Knappett, J., Madabhushi, G., Nikitas, N., Pitilakis, K., Silvestri, F., Viggiani, G., & Fuentes, R. (2020). Seismic behavior of tunnels: From experiments to analysis. Tunnelling and Underground Space Technology, 99. https://doi.org/10.1016/j.tust.2020.103334

Uenishi, K., & Sakurai, S. (2000). Characteristic of The Vertical Seismic Waves Associated with The 1995 Hyogo-Ken NanBu (Kobe), Japan Earthquake Estimated From The Failure of The Daikai Undergrounds Station. Earthquake Engineering and Structural Dynamics, 29(6), 813-821.

Unutmaz, B. (2014). 3D liquefaction assessment of soils surrounding circular tunnels. Tunnelling and Underground Space Technology, 40, 85–94. https://doi.org/10.1016/j.tust.2013.09.006

Vucetic M, & Dobry, R. (1991). Effect of Soil Plasticity on Cyclic Response. J. Geotech. Engrg., 117, 89–107.

Wang, J.-N. (Joe). (1993). Seismic Design of Tunnels A Simple State-of-the-Art Design Approach.

Wang, J.-N., & Munfakhz, G. A. (2001). Seismic design of tunnels. Transactions on the Built Environment, 57.

Xu, Z., Du, X., Xu, C., Hao, H., Bi, K., & Jiang, J. (2019). Numerical research on seismic response characteristics of shallow buried rectangular underground structure. Soil Dynamics and Earthquake Engineering, 116, 242-252. https://doi.org/10.1016/j.soildyn.2018.10.030

Yang, Y., Cao, J., Qu, R., & Xu, Z. (2023). Numerical Simulation of the Seismic Damage of Daikai Station Based on Pushover Analyses. Buildings, 13(3). https://doi.org/10.3390/buildings13030760

Yoshida, N., & Nakamura, S. (1996). Damage to Daikai Subway Station During The 1995 Hyogoken-nunbu Earthqauke and Its Investigation. 11th World Conference on Earthquake Engineering